# EFFECTS OF OPERATING PARAMETERS ON THE PERFORMANCE OF SOLAR WATER HEATING SYSTEMS USING FLAT PLATE AND EVACUATED TUBE COLLECTORS FOR DOMESTIC HOT WATER APPLICATIONS

**Abdi Chimdo**

A thesis submitted to

The Department of Thermal and Aerospace Engineering Program

School of Mechanical Chemical & Materials Engineering

Presented in Partial Fulfilment of the Requirements of the Degree of

**Master of Science in Thermal Engineering**

Office of Graduate Studies

Adama Science and Technology University

Adama

July, 2018

# EFFECTS OF OPERATING PARAMETERS ON THE PERFORMANCE OF SOLAR WATER HEATING SYSTEMS USING FLAT PLATE AND EVACUATED TUBE COLLECTORS FOR DOMESTIC HOT WATER APPLICATIONS

**Abdi Chimdo**

Advisor: **Dr. Chandraprabu Venkatachalam**

Co-Advisor: **Mr. Mebratu Yishak**

A thesis submitted to

The Department of Thermal and Aerospace Engineering Program

School of Mechanical Chemical & Materials Engineering

Presented in Partial Fulfilment of the Requirements of the Degree of

**Master of Science in Thermal Engineering**

Office of Graduate Studies

Adama Science and Technology University

Adama

July, 2018

# Approval sheet

We, the undersigned, members of the Board of Examiners of the final open defence by Abdi Chimdo have read and evaluated his/her thesis entitled "*Effects of Operating Parameters on the Performance of Solar Water Heating Systems Using Flat Plate and Evacuated Tube Collectors for Domestic Hot Water Applications*" and examined the candidate. This is, therefore, to certify that the thesis has been accepted in partial fulfilment of the requirement of the Degree of Masters of Science in Thermal Engineering.

| | | |
|---|---|---|
| ______________________ | ______________________ | ______________________ |
| Supervisor /Advisor | Signature | Date |
| ______________________ | ______________________ | ______________________ |
| Chairperson | Signature | Date |
| ______________________ | ______________________ | ______________________ |
| Internal Examiner | Signature | Date |
| ______________________ | ______________________ | ______________________ |
| External Examiner | Signature | Date |

# Declaration

I hereby declare that this MSc Thesis is my original work and has not been presented for a degree in any other university, and all sources of material used for this thesis have been duly acknowledged.

Name: ________________________________________________________________________

Signature: _____________________________________________________________________

This MSc Thesis has been submitted for examination with my approval as thesis advisor/ Supervisor.

Name: _______________________________________________________________________

Signature: _____________________________________________________________________

This MSc Thesis has been submitted for examination with my approval as thesis co-advisor.

Name: _______________________________________________________________________

Signature: _____________________________________________________________________

Date of submission: ____________________________

# Table of Contents

# Abstract

*This study gives an overview and analysis on the effect of operating parameters on the thermal performance of solar water heating systems with two distinct collector configurations; flat plate and heat pipe evacuated tube collectors. The thermal analysis of these two systems was conducted based on the account of variation in weather conditions of Adama city, volume flow rate, collector orientation and storage tank size, and it was carried out by the virtue of T*SOL® Pro simulation programme.*

*The results showed that for a fluid circulating at 120 l/h, the highest monthly solar fraction of FPC and ETC systems were 80% and 64.6%, respectively, and these values were found around November (Hidar) which have a total solar irradiation of 191 kWh/month. For both systems, the hourly tank outlet temperature was higher during November at 12:00 PM with 87 °C and 71.2 °C for ETC and FPC, respectively. At the end a typical day in April, the energy accumulated in the collectors would reach 2.71 kWh/day for ETC and 2.26 kWh/day for FPC. Regarding the flowrate, simulation of the systems is done for three flow rates (80, 120 and 160 l/h). The results also showed that for a typical day in April, the hourly maximum tank inlet-outlet temperature difference was obtained for both ETC and FPC at 12:00 PM at a flow rate of 160 l/h, where the corresponding maximum tank outlet temperature becomes 74 and 62.5 °C. At this volume flow rate, a solar water heating system efficiency of 59% and 50%, and also a system solar fraction of 82% and 68.1% could be achieved for a SWH system employing ETC and FPC, respectively. For a stationary collector in Adama, the highest solar fraction has been found at a collector inclination of 10° to be 74 and 57.1 for ETC and FPC, respectively. The corresponding mean hourly collector outlet temperature was 40 and 36.2 °C. ETC's energy accumulation in the tank at the end of a year it reached 6074.1 kWh/year, 6266.3 kWh/ year and 6390.5 kWh/ year for 360, 450 and 540 l, respectively, whereas for FPC, it add up to 4836.6 kWh/ year, 5127.93 kWh/ year and 5335.43 kWh/ year, for 360, 450 and 540 l, respectively. The annual system solar fraction for ETC's SWH system is 72%, 74% and 74.1%, for 360, 450 and 540 l, respectively and the system solar fraction for FPC's SWH system is 55.1%, 57.1% and 58.5%, for 360, 450 and 540 l, respectively.*

*Annually, a solar irradiation of 10962 kWh/year will fall on both collectors, and ETC's SWH system lost 3869 kWh/year of this energy at the collector, 760.4 kWh/year at the pipe and 309.4 kWh/year at the storage tank, while FPC's SWH system lost 5094 kWh/year of the collected energy at the collector, 591.5 kW/year at the pipe and 242.4 kWh/year at the storage tank.*

# Acknowledgement

First and foremost my reverence to the glory of Almighty God for enabling me to get this opportunity to successfully carry out my responsibility and complete this study and also for being my strength, comfort and guidance I profoundly needed throughout my study.

Unparalleled gratitude goes to my advisor, Dr. Chandraprabu Venkatachalam. His sharp identification of areas requiring reconsidering and his comments were all constructive in his supervision. His immediate comments and suggestions offered throughout the course helped me complete this study in its present shape. Then, I would also like to thank my co-advisor Mr. Mebratu Yishak for his supervision and support during this work.

I am thankful to the entire academic and administrative teams of ASTU particularly the staff of department of Thermal and Aerospace Engineering program for the tremendous opportunity they gave me to be enrolled in the program, and also for the financial support of the present work.

Last but not least, I would like to thank my dear family members, who did always pray for me and gave their constant moral support, especially my father Dr. Chimdo Anchala for his guidance and encouragement both prior and during this study.

# List of Tables

# List of Figures

# Nomenclatures

| | |
|---|---|
| $A$ | Area [$m^2$] |
| $C_p$ | Specific heat capacity [J/kg K] |
| $I$ | Solar radiation [$W/m^2$] |
| $\dot{m}$ | Mass flow rate [kg/s] |
| $f_{IAM}$ | Incident angle modifier |
| $Q$ | Useful energy collected [$W/m^2$] |
| $T$ | Temperature [°c] |

## *Subscripts*

| | |
|---|---|
| *a* | Ambient |
| *Cm* | Collector mean |
| *d* | Diffuse |
| *dir* | Drect |
| *fi* | Fluid inlet |
| *fo* | Fluid outlet |
| *o* | Overall |
| *p* | Plate |
| *u* | Useful |

## *Acronyms*

| | |
|---|---|
| DHW | Domestic Hot Water |
| ETC | Evacuated Tube Collector |
| FPC | Flat Plate Collector |
| HTF | Heat Transfer Fluid |
| SWH | Solar Water Heater/Heating |

# CHAPTER ONE

# Introduction

## 1.1 Background

Energy plays a pivotal role in our society because of new the life trends which are accompanied with high energy consumption. In a modern society we live in, demand for electric energy is on the rise throughout the world. The tendency of global demand reveals that the emerging economies will begin to require more and more electricity, given their exponential growth. Due to this increasing energy demand, our society has been on the lookout to find different kind's energy sources that are affordable and efficient to meet the specific needs of the people. At the moment, coal, natural gas, woods and oil are among the most used and exploited energy sources. To avoid the harmful effects of these energy sources, we need to find such type of energy source which produce energy as much as conventional fuel like fossil fuel and that source must be not limited. The best option is to use renewable energy. Renewable energy is energy that comes from resources which naturally build up again on a human time scale, such as sun light, wind energy, geothermal heat, rain, tidal energy, wave heat etc. One form of renewable energy is solar energy [1].

Solar energy is heat and radiant light (energy) from the sun. Solar energy technologies produces marketable energy by converting this natural phenomena (sun radiation), into either electrical energy or thermal energy by using solar collectors [2]. The development of solar energy requires accurate estimation of the available solar energy resources and suitable sites for solar collector installations. The generation and distribution of solar energy is highly dependent on the geographical location and topography. Accurate knowledge of the available solar energy resource is very important for the design of any solar-based energy system. This knowledge can significantly contribute to better siting and economic assessment of the new installations, monitoring of their performance and forecasting of delivered energy [3]. Ethiopia has abundant solar energy resources. The national daily average irradiance is estimated to be 5.2 $kWh/m^2/day$ with seasonal variations that range between the minimum of 4.5 $kWh/m^2/day$ in July to a maximum of 5.6 $kWh/m^2/day$ in February and March. The solar resource is relatively lower in the most populous Northern, Central and Western highlands of the country while the rift valley regions, western and eastern lowlands of the country receive higher annual average irradiance well above 6 kWh/$m^2$/day [4].

Solar Water Heating (SWH) systems installed in Ethiopia are mostly simple and modular collectors with separate water tanks. An estimated 80% of total installed capacity of SWHs is within Addis Ababa. It is estimated that the residential housing SWH market takes the lion's share of 90 % while the surplus goes to hotels and tourism. The SWH market was started with locally manufactured products and is currently entirely based on imported products. The market for solar water heaters started with locally manufactured products about a decade ago but currently, local manufacturing has been squeezed out of the market for it could not compete with cheaper but higher quality imported products so, the market nowadays is entirely based on imported products. The country's predominant operator model in the SWH industry is known for companies that engaged in importation, retail, installation and maintenance. Technologies available in the market range from simple flat plate collectors to evacuated tube with heat-pipes. Currently, there are about seven companies that import and sell SWHs in large volumes [4].

The proper design of SWH systems is important to assure good performance. There are many studies in the literature that address the design method of these systems. These design methods can be broadly classified into two categories, namely, correlation-based methods and simulation-based methods. The typical correlation based methods include the $\phi$ method and f-chart method. These design methods have been widely used in preliminary design due to their convenience and inexpensiveness in predicting long-term performance compared to detailed simulation-based methods. The application of these design methods, however, is limited, particularly when the meteorological data and the usage characteristics of the SWH system are different from the data used for corrections [5]. On the other hand, a number of simulation-based methods such as TRNSYS, T*SOL and SOLCHIPS have been applied for the design of SWH systems and are also available on the market as user-friendly software tools. Researchers and designers can numerically evaluate the effects of design variables on long-term energy performance by conducting a series of simulations. These design variables could include the collector area, number of the collectors, storage tank volume, auxiliary heater capacity, and number of the auxiliary heaters. However, even one of these design variables could cause a variation in the SWH system's performance. Therefore, the number of simulations increases exponentially according to the increase in the number of design variables and parameters.

Moreover, these methods also require the involvement of experts and significant computation time [6].

## 1.2 Problem Statement

While solar water heating systems have the potential to provide the majority of household hot water and to lower carbon emissions, yet it's only recently that these systems started to be introduced to a developing city like Adama. Thus, like any other upcoming technology, there can be some uncertainties among residents of the city regarding the effects of various operating variables on energy production from small-scale (domestic) solar collector installations. Due to this reason, most consumer's goal is largely aimed only at subsidizing purchase and installation on the assumption that these are sufficient steps towards constructing a system that can meet the required hot water demand efficiently. The subsequent analysis provides evidence to the contrary because, without having the proper understanding on the system's sizing (for system components and operating parameters) and how they should be operated, it would be impossible to build a system, one that operates using its full potential. Investigation on areas of performance improvement would provide the local consumers of these technologies with an essential knowledge to build a more efficient domestic solar water heating system.

## 1.3 Objectives

### 1.3.1 General objective

The main objective of this thesis is to investigate the effect of different weather conditions of Adama city, inclination angles, volume flow rate, and system sizes on the performance of domestic solar water heating systems that uses flat plate and heat pipe evacuated tube collectors, and also to compare the performance of these two systems with each other, based on thermal analysis.

### 1.3.2 Specific objectives

The specific objectives of this thesis are:

- To give a brief overview on areas that can be seize to improve the thermal performance of domestic solar water heating systems.
- To perform the simulation of the two SWH's systems using T*SOL pro 5.5 software

based on thermal analysis with different weather conditions, inclination angles, volume flow rate, and storage tank sizes to study the impact of these operating conditions on the system efficiency, system solar fraction, storage tank outlet temperature, collector outlet temperature, energy accumulated and collected in the tank and collector.

- To investigate the overall thermal losses of the two solar water heating systems.

## 1.4 Significance of the Study

The main significance of this project is to provide any local person who is interested in using solar water heating technologies, with the necessary informations required to select the most appropriate solar collector system and its operating conditions. The proper selection and employment of SWHs that can solve a problem that our community faces regarding the shortage and rise of energy cost.

## 1.5 Scope and limitation of the Study

***Scope***

This project is intended to investigate and compare the effect of various operating elements on the thermal performance of heat pipe evacuated tube and flat plate collectors.

***Limitations***

i. Currently available SWH simulation softwares (TRNSYS, TSOL and PolySun) doesn't provide the option to alter the characteristics of the constructing elements of a collector like; number of tubes, absorber plate thickness, glazing type and insulation thickness and others, thus are not included in this study.

# CHAPTER TWO

# Literature review

## 2.1 Overview of Solar Water Heating systems

The idea of using solar energy collectors to harness the sun's power is recorded from the prehistoric times when at 212 BC the Greek scientist/physician Archimedes devised a method to burn the Roman fleet. Amazingly, the very first applications of solar energy refer to the use of concentrating collectors, which are by their nature (accurate shape construction) and the requirement to follow the sun, are more 'difficult' to apply. The interest for water and house heating appeared in the mid-1930's, but gained interest in the last half of the 40's. Until then millions of houses were heated by coal burn boilers. The idea was to heat water and fed it to the radiator system that was already installed. The manufacture of solar water heaters (SWH) began in the early 1960's. Since then, the industry of SWH's have expanded very quickly in many countries of the world. The greatest advantage of solar energy as compared with other forms of energy is that it is clean and can be supplied without any environmental pollution. In addition to the thousands of ways in which the sun's energy has been used by both nature and man through time, to grow food or dry clothes, it has also been deliberately harnessed to perform a number of other jobs such as; to heat and cool buildings, to heat water for domestic and industrial uses, to heat swimming pools, to power refrigerators, to operate engines and pumps, to desalinate water for drinking purposes, to generate electricity, for chemistry applications, and many more [7]. Two types of active solar energy systems can be used to heat domestic and service hot water:, direct circulation and indirect. These are called active systems because a pump or fan is employed in order to circulate the fluid.

### 2.1.1 Direct circulation systems

In direct circulation systems, shown schematically in Fig. 1, a pump is used to circulate potable (drinkable) water from storage to the collectors when there is enough available solar energy to increase its temperature and then return the heated water to the storage tank until it is needed. As a pump circulates the water, the collectors can be mounted either above or below the storage tank. Direct circulation systems can be used in areas where freezing is not frequent. For extreme weather conditions, freeze protection is usually provided by recirculating warm water from the storage tank. Direct circulation systems often use a single storage tank equipped with an auxiliary water heater, but two-tank storage systems can also be used. Direct circulation systems can be used with water supplied from a cold water storage tank or connected directly to city water mains. Pressure-reducing valves and pressure relief valves are required however when the city water pressure is greater than the working pressure of the collectors. Direct water heating systems should not be used in areas where the water is extremely hard or acidic because scale deposits may clog or corrode the collectors.

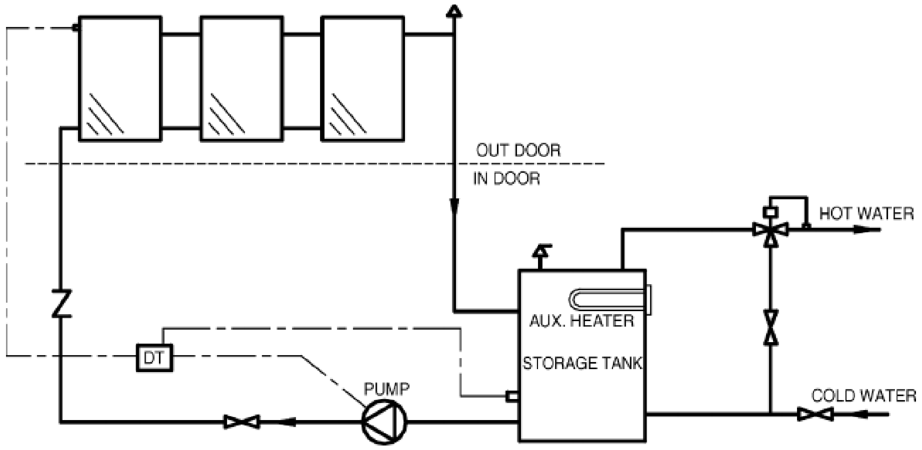


Fig. 29. Direct circulation system.

Figure 1. Direct circulation system *[Kalogirou]*

### 2.1.2 Indirect water heating systems

Indirect water heating systems, shown schematically in Fig. 2, circulate a heat transfer fluid through the closed collector loop to a heat exchanger, where its heat is transferred to the potable water. The most commonly used heat transfer fluids are water/ethylene glycol solutions, although other heat transfer fluids such as silicone oils and refrigerants can also be used. When fluids that are non-potable or toxic are used double-wall heat exchangers should be employed. The heat exchanger can be located inside the storage tank, around the storage tank (tank mantle) or can be external. It should be noted that the collector loop is closed and therefore an expansion tank and a pressure relief valve are required. Additional over-temperature protection may be needed to prevent the collector heat transfer fluid from decomposing or becoming corrosive [1].

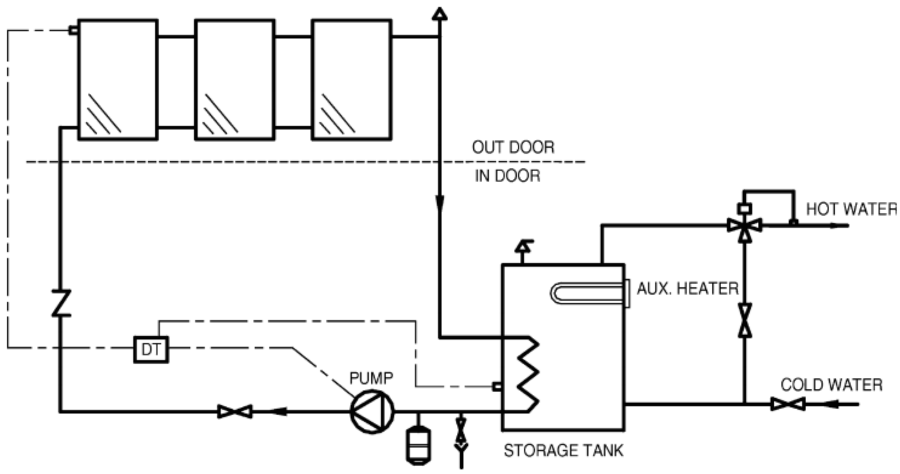


Figure 2. Indirect water heating system *[Kalogirou]*

## 2.2 Solar thermal collectors

Solar collectors are devices that are used to harness the energy from the sun, converting the incoming solar radiation into useful heat energy. Being the key element in solar energy utilization systems, solar energy collectors act as heat exchangers that converts the solar radiation energy into internal energy of the transport medium. The solar energy will be collected by absorbing the incoming solar radiation and converting it into heat, and transferring this heat to a fluid. Then, this heat energy will be transferred from the fluid to the heat application processes or the storage tank [9].

There is a high consumption of non-renewable primary energy for domestic hot water systems. Therefore, a potential solution is needed for the accelerating surge in the share of the energy demand. This led to development of energy-saving technologies and the use of renewable energy sources such as solar energy [2]. Solar energy collectors are basically distinguished by their motion, i.e. stationary, single axis tracking and two axes tracking, and the operating temperature. Stationary solar collectors are permanently fixed in position and do not track the sun. Three types of collectors fall in this category are Flat plate collectors (FPC), Stationary compound parabolic collectors (CPC) and Evacuated tube collectors (ETC) [1].

Exergy analysis has been performed for different types of solar collectors. Most of it is in the field of flat-plate solar collectors. The second most popular area of study refers to combined photovoltaic and thermal collectors. Also, a few studies has been done on parabolic trough collectors and evacuated tube collectors too. Parabolic dish collectors have been analysed and optimized by a number of researchers and showed to have high exergetic efficiency. Other types of collectors less often researched are compound parabolic collectors, heat pipe collectors and cavity receivers [9].

The energy generated by a solar collector is dependent on the angle at which it is tilted and the orientation of the solar collector. For maximum energy gain, solar panels should be inclined at optimal tilt angle and seasonal adjustment of the panel may lead to considerable gain in energy obtained from solar energy. The optimum North – South tilt angle and East- West orientation angle is different for each months of the season and shows variation in the direction of sun with time of day and month of the season. The collected solar energy will be greater if we choose the optimum panel tilt for the season [8].

### 2.2.1 Flat plate collector

Flat plate collectors (FPCs) are primarily composed of a glass cover, absorber plate and insulation material. The glass cover is used to trap the hot air by reducing the radiation and convection losses to the surrounding, the absorber plate has tubes filled with the working fluid whereas the insulation material is used to reduce conduction losses. For flat plat collectors, the materials, the dimension, number and size of tubes and number of glass covers can vary for different application and are selected based on the chosen criteria of the specific application [10]. A typical flat-plate solar collector is shown in Fig. 3.

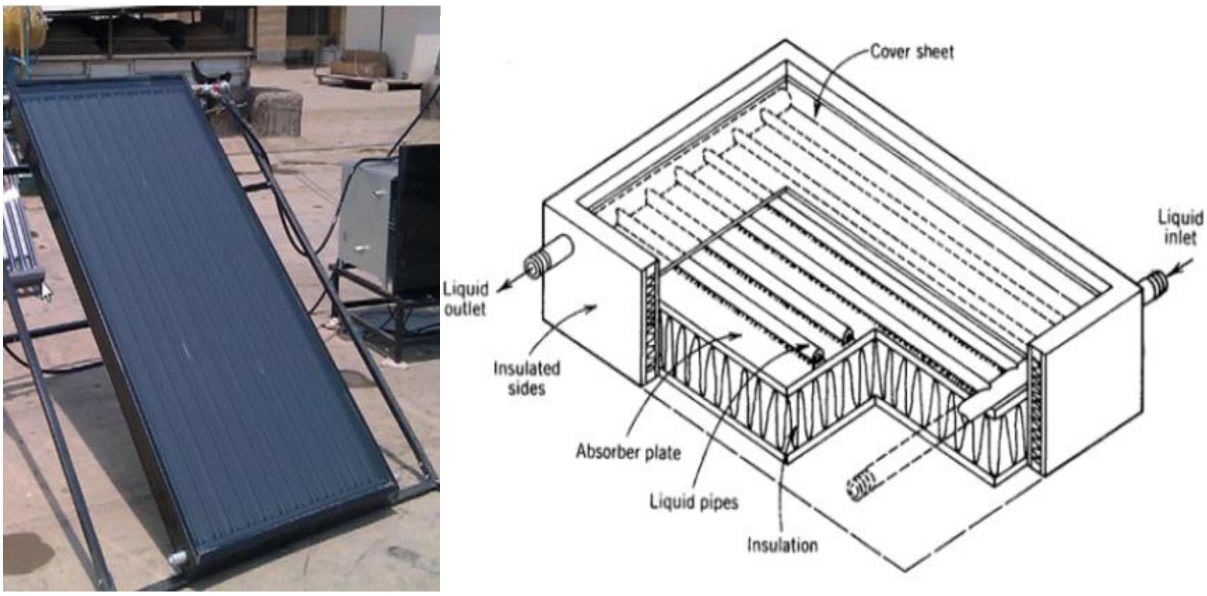


Figure 3. Pictorial view and sectional view of flat plate collector *[Farzad and Emad]*

Addisu et al. [11] investigated the potential use of solar energy for large-scale water heating systems on four selected sites; Addis Ababa tannery, Dire tannery, Ethiopian tannery and

Jimma hospital, Ethiopia. The transient analysis was performed for a 2 $m^2$ flat plate collector and the system gave a corresponding solar contribution to the heating load and a maximum solar fraction of 1 and 80.9% for Addis Ababa tannery; 0.981 and 76.2% for Dire tannery; 0.91 and 81.6% for Ethiopian tannery; and 0.975 and 81.8% for Jimma hospital, thus proving solar energy can be used for large-scale water heating systems in Ethiopia.

A new approach have been proposed that improves the hot water production from flat plate collector. The optimization of the thermal energy efficiency was guaranteed by using an electronic architecture that controls the mono-axial tracker. The electronic system dedicated to the control and command consumes an average of 278.2 Wh/day. From 7:00 to 9:30 AM, the FPC receives a remarkable quantity of solar radiation equal to 1040W, while the stationary FPC receives an average of 531W. This improvement of solar radiation collection influences directly on the hot water production performance, allowing the improved FPC to produce an average of 719 W, while the stationary FPC produces 353 W [12].

By increasing the mass flow rate of the working fluids we can increases the efficiency of the flat plate collector. Water gives a lower efficiency at lower flow rates but for a flow rate of 0.016 kg/s and above, since the pumping power adversely affects the thermal efficiency of the collector, at the turbulent flow conditions water becomes more efficient HTF [13].

The investigations on the performance of FPC were done for two different two climatic conditions with TRNSYS software. In order to get suitable outlet temperature (70 to 90 °C) they used three collectors which are connected in series. Based on the study the thermal efficiency is increased with increasing the inlet temperature. So the first collector has more useful energy gain (3775 kJ/hr) than the second one (3300 kJ/hr) also, the useful energy gain is more than from the second one is more than the third one (2825 kJ/hr) [14].

Weiqiang et al. [15] introduced a dynamic test method is which is an improved transfer function method that features on two new collector parameters. One is time term which can indicate solar collector's inner heat transfer ability and the other is a second order term of collector mean fluid temperature which can obtain fluid thermal capacitance in data processing. It was concluded that, the improved transfer function method can accurately and stably estimate flat plate solar collector under dynamic test conditions with correct test procedure and data processing method.

In order to improve the performance of the solar energy collectors, a reflector was introduced. It was observed that the collector efficiency and heat transfer rate depend on solar radiation.

The collector efficiency, without reflector is about 51%, but this can be maximized by 10% to an efficiency of 61% by mounting a glass to prevent the radiation emitted by the absorber plate from escaping, and using a reflector to concentrate the solar heat on the collector [16].

Lacour et al. [17] carried out the year round performance analysis of two commonly of two commonly installed forced circulation SWH systems in temperate climates has been carried out using trial installations. Results obtained show that for an annual total in-plane solar insolation of 1087 kWh/m2, a total of 1984 kWh of heat energy were collected by the 4 m2 FPC system. Over the year, a unit area of the FPC generated 496 kWh/m2 of heat. For 3149.7 kWh of auxiliary energy supplied to the FPC system, its annual solar fraction was 38.6%. The annual average collector efficiency was 46.1% and 60.7% while the system efficiency was 37.9%. Chandraprabu et al. [18] has studied the performance of CuO/Water nanofluid instead of water as an outer fluid in the tube of condensing unit of air conditioner.

### 2.2.2 Heat pipe evacuated tube collector

Heat pipe evacuated tube collector (ETC) contain two glass tubes made of borosilicate where the inner and outer glass tubes are separated by vacuum space. The vacuum plays the role of an insulator to block the short wave radiation from escaping and this has proven to be the best methods to trap radiation. It is also used to direct the radiant energy incident inside the tube without a huge heat loss. These solar collectors consist of a heat pipe inside a vacuum-sealed tube, as shown in Fig. 4. The pipe, which is a sealed copper pipe, is then attached to a black copper fin that fills the tube (absorber plate). Protruding from the top of each tube is a metal tip attached to the sealed pipe (condenser). ETC use liquid – vapour phase change materials to transfer heat at high efficiency. The heat pipe contains a small amount of fluid (e.g. methanol) that undergoes an evaporating-condensing cycle. In this cycle, solar heat evaporates the liquid, and the vapour travels to the heat sink region where it condenses and releases its latent heat. The condensed fluid return back to the solar collector and the process is repeated. When these tubes are mounted, the metal tips up, into a heat exchanger (manifold). Water, or glycol, flows through the manifold and picks up the heat from the tubes. The heated liquid circulates through another heat exchanger and gives off its heat to a process or to water that is stored in a solar storage tank [19].

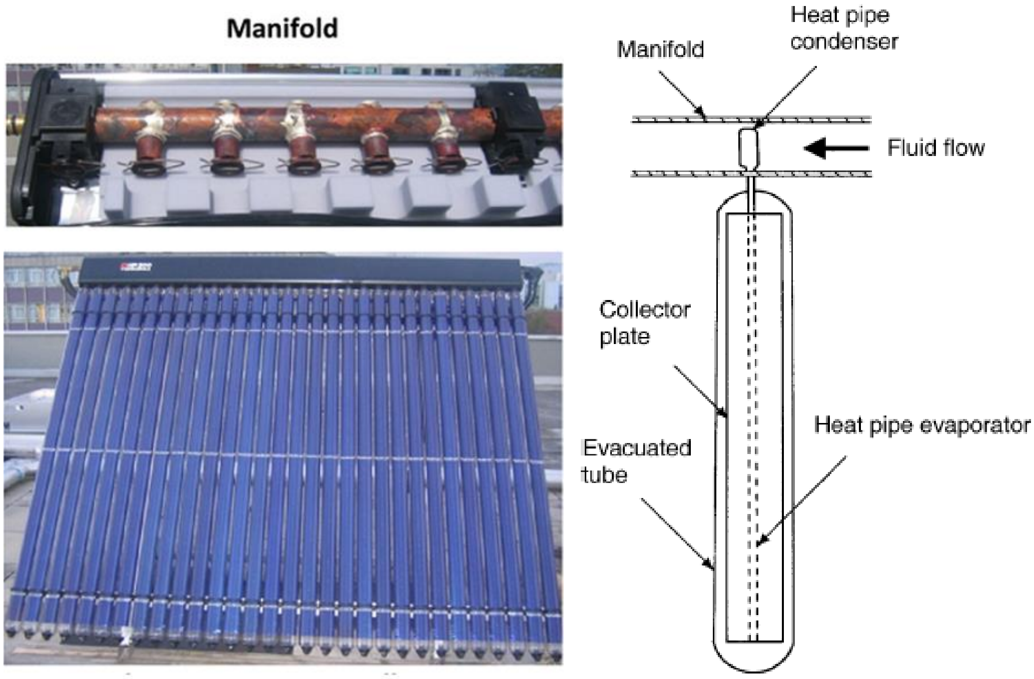


Figure 4. Pictorial view and sectional view of heat pipe evacuated tube collector.

Evacuated tube collector is preferably used for high temperature applications such as desalination of sea water, air conditioning, refrigeration, and industrial heating processes since their performance is better than that of Flat Plate Collectors [20].

Evacuated tube solar collectors (ETC) are the most widely used type of collectors because they have a high working temperature and thermal efficiency compared to other collectors such as flat plate solar collectors. The efficiency of evacuated tube collector can be increased by using a heat pipe as the absorbing element in the collector tube. The heat is transferred through the heat pipe having a small temperature difference of fluid between the heat input and output. The heat pipe consists of a closed container integrated with a capillary device then charged with a working fluid suitable for the operating conditions. The fluid first gain a latent heat of vaporization in the pipe, and then it vaporizes in the manifold [21].

Xianhua et al. [22] stated that, higher thermal efficiencies can be achieved for the evacuated tube solar collectors by the reducing the inlet fluid temperature. For temperatures below zero, the thermal efficiencies increase as the reduced temperature decreases, and the growth rate of the thermal efficiency will decreases slowly. The growth rate of the thermal efficiency is higher for lower solar irradiances which are the higher sensitivity to the mass flow rate and the solar irradiance changes.

The heat collecting efficiency of evacuated tube solar collector is conducted by the simulation method. The results show that the annual average heat efficiency of the evacuated tube solar water heating system is 42.9%. The heat efficiency of ETC was the largest in August, and the lowest in December, which goes to show that the air (ambient) temperature has great influence on the heat collecting efficiency of the collector [23].

A two part experiment, one for the evacuated tube collector/storage with a compound parabolic concentrator and one without a compound parabolic concentrator were conducted by Piotr and Robert [24] to measure the heating medium flow rate and solar radiation intensity using a flow meter and pyranometer, respectively. They found that for the first 80 minutes, the paraffin's temperature increased steadily for the evacuated tube collector/storage with a compound parabolic concentrator and without it, but soon, the CPC showed to have an effect on the rise of the temperature causing the temperature of the paraffin to rise more rapidly. The main reason for this is the fact that the CPC will direct more solar radiation on the surface of the evacuated tube.

After conducting an investigation on $2m^2$ concrete absorber plate solar water heater, Ajinkya [25] stated that, during months of September, January and April average water temperature of 150 *l* of water collected per day is found to be 62 °C, 59 °C and 69 °C respectively at a water flow rate of 30 *l*/h. Thus, with this capacity of the evacuated tube solar water heater, it is possible to fulfil the demand of hot water for various purposes in most weather conditions mostly for normal weather days and partially, for cloudy days.

From the thermal standpoint, the ambient conditions selected for the design will determine the number of solar collectors required to attain the targeted performance from the system. Larger collector areas can be used to compensate for certain deficiencies such as lower inlet temperatures and a lower solar radiation intensities [26].

Rigardt et al. [27] developed a numerical model and implemented EES (Engineering equation solver) to investigate the performance of a SWH system using a heat pipe evacuated tube collector. Results from the analysis showed that for a city that is located in South Africa in summer, a 40° slope produced the least amount of useful heat and outlet temperature, whereas the 25° slope produced the most. In winter, the opposite was observed, and the 40° slope produced the greater amount, thus showing the dependency of optimal collector angle on a season.

To increase the outlet temperature of the working fluid it's recommended to lower the mass flow rate of the fluid and use optimum length of collector. The net heat energy gain at high solar intensity is highly affected by the change in the ambient temperature. Based on the study, water has proven to be the best heat energy absorber fluid compared to air and LiCl-$H_2O$ solution [28].

Dimitri et al. [29] investigated the performance of evacuated tube collectors and flat plate collectors having equal gross surface area (2 $m^2$) in Nordic climate condition of Estonia. The testing of solar collectors was held from August to September and March to April. On rainy and cloudy days, ETC produced 21-64% more energy than FPC and using solar trackers increased the productivity of ETC by 41%.

## 2.3 Sizing a Solar Water Heating (SWH) system

Sizing a solar water heating system is by determining the collector area that will meet the heating load, depending upon the irradiation level and in some cases, the collector area that will give maximum life cycle solar savings (minimize life cycle cost) of SWH system [30]. It is therefore possible to minimize life-cycle cost by sizing a system that meets 100 percent of the load on the sunniest day of the year. SWH system sizing also involves the determination of the required storage tank capacity to provide an energy buffer between periods of low irradiation levels such as night and cloudy days, and periods of high irradiation levels. Pumps can be selected according to the recommended flow rate of the fluid in the collector as specified by the collector manufacturer [31].

### 2.3.1 Collector choice, surface sizing and orientation

Selecting the right collector is the most important factor in building a solar water heating system. For seasonal pool heating, cheaper collectors of worse thermal properties will be sufficient, for prolonging a bathing season to the spring and autumn, collectors for all year operation shall be used (black chrome or Sunselect surface), as well as in case when all-year solar-heated DHW and additional heating is desired. For better energy gains or for operation under extreme temperatures, the best solution is using tube collectors, especially the versions with many tubes without mirrors bring energy gains even from diffuse radiation, i.e. during cloudy periods (diffuse radiation is reflected only very little by mirrors). A calculation of a collector surface size always comes out from the heat quantity needed and the period in which this need shall be covered. The energy needed is then compared to the average quantity of solar energy received by one square meter in the period in question, decreased according to the solar system efficiency. The result is the size of collector surface needed, possibly increased by an index in case of adversely oriented collectors, which is finally re-calculated to the number of collectors needed. Solar collectors are usually calculated to cover 100% of DHW need in the period between April and August. The orientation of a collector with respect to the South and its inclination (the angle from a horizontal plane) represents another factor influencing the total energy balance [32].

### 2.3.2 Daily hot water consumption

Estimation of hot water consumption is a difficult task because the consumption pattern (profile) depends on many variable factors difficult to quantify such as living standards, gender and purpose of the building. ASHRAE [35], recommends hot water consumption of 75 litres per day per person. Also, according to the National Renewable Energy Laboratory (NREL) of the US Department of Energy, a workshop on solar thermal technology and applications by Roger Taylor [36] provided the following values for hot water usage in various types of buildings in Table 1.

Table 1. Typical hot water usage in buildings [36]

| Type of building | Consumption per occupant |
|---|---|
| Dormitory | 49 litre per day per person |
| Motel | 57 litre per day per room |
| Hospital | 68 litre per day per bed |
| Office | 4 litre per day per person |
| Food Service | 9 litre per day per meal |
| Residence | 75 litre per day per person |
| School | 7 litre per day per student |

### 2.3.3 Required storage tank capacity

The size of the storage tank affects the outer surface area and hence affects the tank’s heat loss conductance. The storage tank can be sized according to the total collector area and the daily heating load requirements [23]. When sizing a DHW tank or an accumulation tank, usually a size for 1-1.5 day heat consumption is used. For DHW tanks, sizing comes out from the number of persons to be served, the usual size of a tank for calculations is 75 litres per person [33]. Duffie and Beckman [30] recommends tank capacities ranging from 50 to 200 litres per square metre of collector for an annual system performance to be insensitive to tank capacity. Due to an unstable energy supply from the sun, it is advisable to oversize the tank a little bit.

### 2.3.4 Estimating total heating load

The loads to be met by a solar water heating system are generally grouped into two; hot water load and heat losses from tank and piping. The heat losses from the tank and piping are estimated as a fraction of the total hot water load [34]. If the total daily need of hot water is known, the heat required to heat it up can be calculated by the popular equation $Q=mc\,(T_2-T_1)$.

## 2.4 Factors affecting SWH systems performance

### 2.4.1 Weather conditions

The amount of incident radiation determines the absorbed solar radiation by the collector while the ambient temperature determines the thermal losses from the collector. Cloudy conditions limit the beam radiation levels and thus the radiation absorbed by the collector especially the concentrating collectors [31].

### 2.4.2 Collector orientation and tilt

Geographic orientation and collector tilt can affect the amount of solar radiation the system receives. Collector orientation is critical in achieving maximum performance from a solar energy system. In general, the optimum orientation for a solar collector in the northern hemisphere is true south (azimuth of 180°) as illustrated in Fig. 5. However, recent studies have shown that, depending on the location and collector tilt, the collector can face up to 90° east or west of true south without significantly decreasing its performance. The Optimum tilt angle for solar collector is an angle equal to the latitude [30].

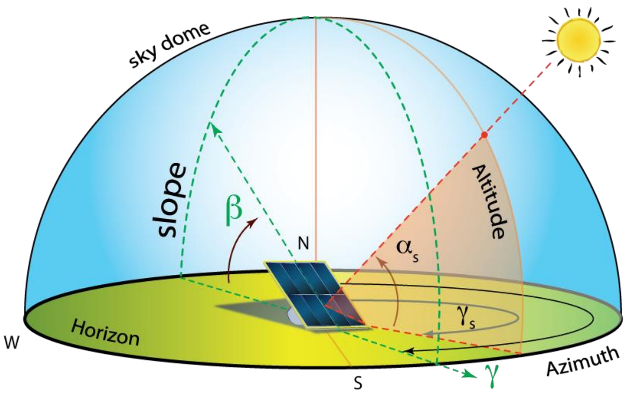


Figure 5. Collector orientation in the Northern Hemisphere

### 2.4.3 Transport fluid flow rate

Low collector fluid flow rates increases the thermal performance of the collector by increasing the degree of storage tank thermal stratification. In a stratified tank, the temperature of fluid at the bottom of the storage tank is lower than at the top. Collector inlet temperature is reduced because the collector inlet fluid is fed from the bottom portion of the tank. Lower inlet collector temperature reduces thermal losses. This results in increased useful energy gain.

### 2.4.4 Collector array arrangement and characteristics

Collector area and its glass cover optical properties affect the amount of the incident solar irradiation that can be absorbed while collector insulation thickness and its thermal conductivity affect the overall heat loss coefficient and thus the thermal losses. The performance of the collector array depends on how the collector modules are connected. In parallel connection, module inlet and outlet ports are fed to the common respective headers. Assuming identical modules, fluid inlet temperature is the same to all modules in the array. This is also true to fluid outlet temperature. The performance of the collector array is thus the same as the performance of the individual collector. In series connection, the performance of the second and subsequent modules will not be the same as the first because its inlet temperature is the outlet temperature of the first [30].

### 2.4.5 Working fluids

For effective heat transfer, the fluid should be stable at high temperatures, noncorrosive and safe. It also should be cost-effective. Air is attractive for heating and cooling applications. However, the heat transfer is very poor. The most commonly used working fluids are pressurized water, liquid metals, therminol 55, and Mobile therm 603 [37]. Water based fluids can be either pure water or a water and glycol mixture with either ethylene or propylene glycol which are types of “antifreeze”.

***Distilled water***

Distilled water has been suggested for use in solar collectors since it avoids some of the problems of untreated potable water. Since the distillation process removes contaminants such as chlorides and heavy metal ions the problem of galvanic corrosion should be eliminated. However, distilled water is still subject to freezing and boiling. For this reason glycol-water concentrations are most preferable [38].

***Glycol-water antifreeze***

Non-freezing liquids can be used to provide freezing protection. These liquids are circulated in a closed loop with a double wall heat exchanger between the collector loop and the storage tank. In this part there is only a description of the antifreeze solutions and their properties. Water-Glycol antifreeze solutions are the most commonly used because their cost is less compared to silicon fluids. Ethylene and propylene glycol are the two most common antifreeze solutions. A concentration of 50% ethylene or propylene glycol and 50% water solution provides freeze protection to about -20°C. The boiling point also rises to about 120°C [38].

The use of glycol-water solutions has the disadvantage of corrosion. Glycol-water solutions corrode galvanised pipes and at high temperatures glycols may break down to form glycolic acid. This break down usually occurs at 85°C and accelerates as the temperature reaches 95°C. This glycolic acid corrodes almost all the metals used in solar collectors including copper aluminium and steel. The decomposition rate of glycol varies according to the degree of exposure to air and the service life of the solution.

Most glycol-water solutions require periodic monitoring of the pH level and the corrosion inhibitors. The appropriate value of pH is between 6.5 and 8.0. Also the replacement of the solution is done every 12-24 months or even sooner in high temperature systems. Table 2 shows the physical properties of water and water glycol mixture at a mean temperature of the fluid.

Table 2. Physical properties of heat transfer fluid [38]

| **Fluid** | **Temperature (°C)** | **Density (kg/m³)** | **Viscosity (g/ms)** | **Specific heat (kJ/kg °C)** | **Thermal conductivity (W/m °C)** |
|---|---|---|---|---|---|
| Water | 38 | 993 | 0.684 | 4.166 | 0.628 |
| | 93 | 963 | 0.305 | 4.208 | 0.661 |
| Ethylene glycol and water, 50 % by weight | 38 | 1054 | 2.3 | 3.43 | 0.398 |
| | 93 | 1016 | 0.76 | 3.64 | 0.433 |

## 2.5 Conclusion of literature review

This study presented the review of flat plate and evacuated tube collectors. Applications and processes include the use of phase change materials either in the collection or storage of thermal energy, heating, solar cooling, drying, domestic cogeneration, solar assisted heat pumps and others. Here, the utilization of solar thermal collector's specifically focuses on solar water heaters which undertake the conversion of solar energy into thermal energy (heating).

The general conclusions of the review are

- The performance of solar water heater systems depend on the mass flow rate of the heat transfer fluid.
- Weather conditions (Air temperature, solar intensity and wind speed) in which the system is located or installed also affect the performance of solar water heating systems.
- A calculation of a solar water heating system's size always comes out from the heat quantity needed and the period in which this need shall be covered (hot water consumption profile).

# CHAPTER THREE

# Simulation setup

## 3.1 Simulation software

In this study, the T*SOL® Pro 5.5 (R6) analysis tool is used for analysing the solar water heating system. T*SOL® is a dynamic software programme used to simulate and optimise solar thermal systems such as hot water systems and space heating applications. This is preferred to other analysis tools because it has an integrated MeteoSyn tool which allows users to create climate data for locations outside of the included data base. It also requires input parameters such as project climate data location, system consumption, collector type selection and system configuration selection to automatically size the collector and storage tank. It provides project report, economic analysis, efficiency calculation and annual simulation of the system as output [39]. The assessment of the DWH systems will be based on the first law of thermodynamics. The results are determined by a mathematical model calculation. Actual yields can deviate from these values due to fluctuations in climate, consumption and other factors.

The T*SOL® software programme accepts the following parameters as inputs; weather data, average daily hot water consumption, desired hot water temperature, type of collector, tank capacity, slope of collector, collector azimuth angle and cold water temperature. The programme outputs the following;

i. Total annual global solar irradiation in the plane of the collector and fraction of diffuse component of solar irradiation.
ii. System components in terms of required number of collectors, total gross collector area, total collector aperture (active) area, collector surface area irradiation, annual circulation losses, volumetric flow rate per $m^2$ of collector area and collector manufacturer.
iii. Thermal performance in terms of the resulting annual energy requirement, annual system energy losses, energy produced by collector and collector loop, contribution of solar to annual energy requirement, energy from auxiliary heating, solar fraction and system efficiency.

## 3.2 Operational sequence of T*SOL simulation software

A simplified operational sequence for the simulation of a thermal solar water heating system with T*SOL looks like the following:

1.  **Create new project or new variant:** After starting T*SOL, it's possible to create a new project, open the last project edited or select another project (if it already exists). Within a project, one can create any number of system variants and edit up to eight of them at one time.

2. 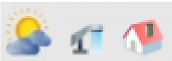 **Set weather and site data:** In order to design a useful solar system, the climatic conditions in which it operates and its site data must be known.

3.  **Set hot water consumption:** The DHW requirement and its distribution over the year are key values for simulating a solar system. At the same time, the total consumption for the operating time and the resulting energy requirement are displayed. The weighted consumption profile is displayed as a graph and a table for every day of the week, the entire week, and the year.

4.  **Select system:** On starting, one must first select a system. The system is the solar system that is selected with a predefined collector loop configuration, storage loop with corresponding tank type, consumption loop, and the associated control strategy. The separate components can be exchanged in the system definition.

5.  **Define component parameters:** The systems are made from individual components. Define or modify the properties of these components in the relevant dialog. Go through all the components in this system and enter the required parameters.

6.  **Run simulation:** After setting the parameters of the solar system, it's now possible to simulate its operational state over the period of a year. The simulation is carried out for the project's active variant.

## 3.3 Weather data

For this study, the solar radiation, ambient temperature and wind speed of Adama, Ethiopia ($8.33^0$ N and $39.17^0$ E) was selected from the MeteoSyn tool database, and based on this data, the simulation analysis was done on each hour, day and months of a year. APPENDIX A shows tables of mean hourly, daily and monthly values of ambient air temperature, solar radiation and wind speed of Adama city.

## 3.4 DHW consumption profile

The DHW requirement and its distribution over a year are key values for simulating a solar system. The monthly average hot water consumption is roughly constant across a year. For this study. Adama's daily load pattern used for the load cycle simulations was adopted for detached house (Single-family dwelling), together with the simulation software's automated hot water draw off system to mimic domestic hot water use. The amount of hot water needed for a particular household is based upon how much hot water is typically used per day.  An average household in Adama uses about 75 L of hot water per person per day and according to the Ethiopia Rural Socioeconomic Survey (ERSS) [42], Ethiopia's average household size is 5.1 persons. This means, for a family of five, the total daily hot water consumption will be 375 *l*. Fig. 6 shows the profile of the daily domestic hot water demand.

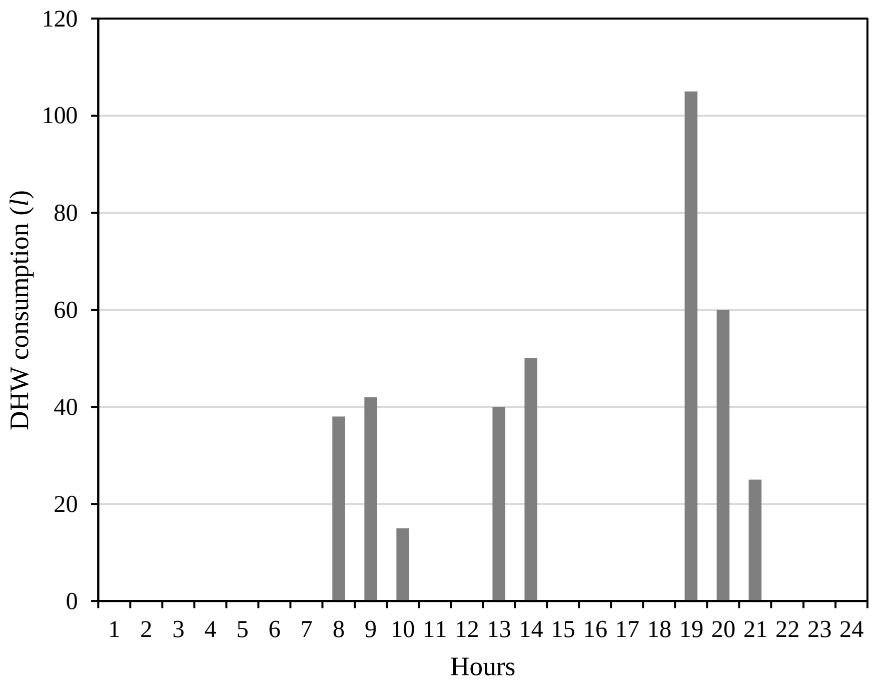


Figure 6. DHW consumption at different times of a particular day

## 3.5 Description of the SWH systems

An indirect active system was selected as the basis for the design of the systems. The main components of the SWH system includes solar thermal collector, controller, electric pump and storage tank. A schematic diagram of the examined water heating systems is shown in Fig. 7.

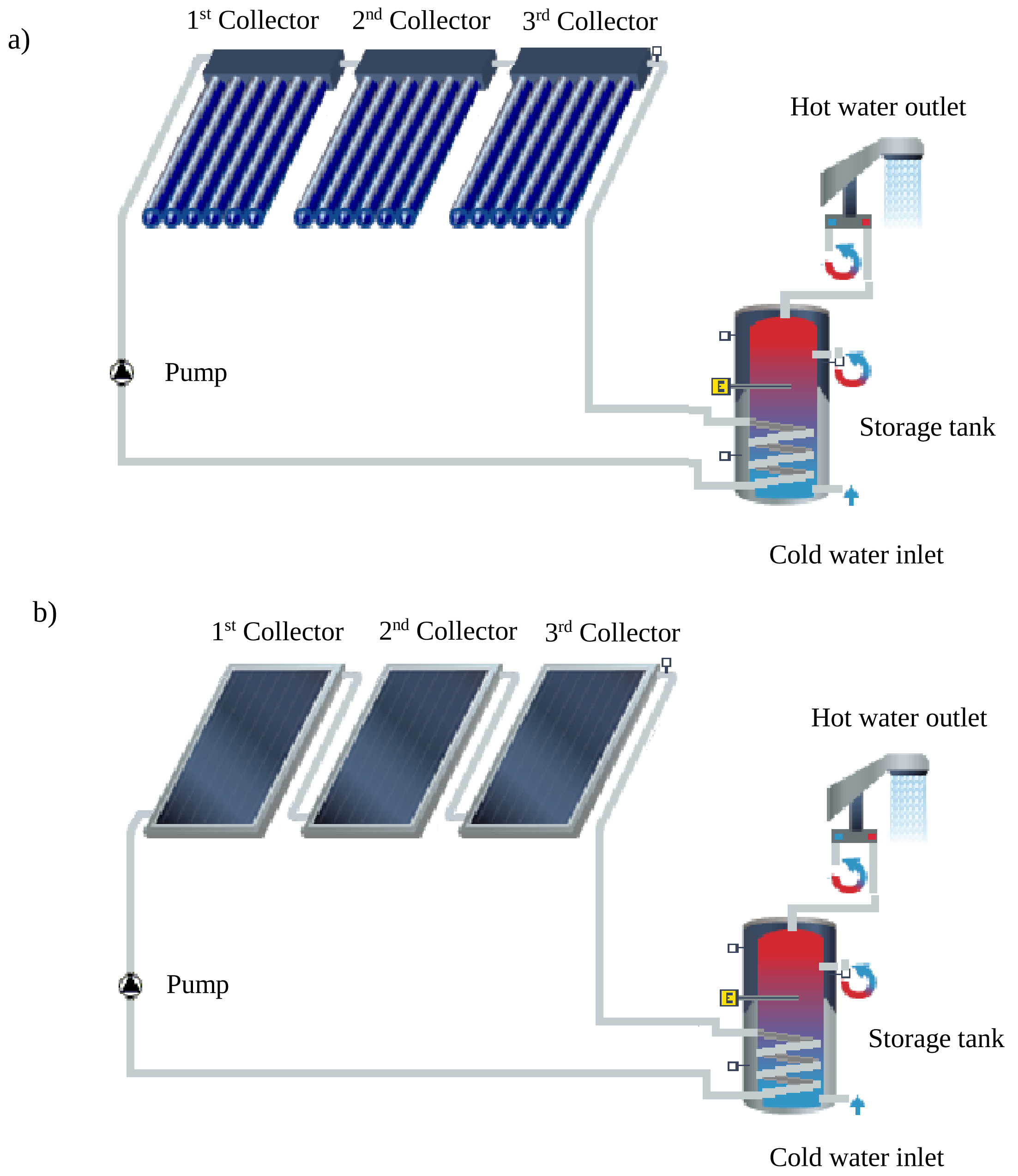


Figure 7. Schematic diagram of a) ETC and b) FPC SWH systems

### 3.5.1 Thermal collector

T*SOL® provides up to date database of many certified solar collectors which are tested according to the Solar Collector Certification Program (SRCC) and certified by independent institutes. Out of those collectors, the type KSC-AE/200/S and OPC 15 are selected for the simulation representing the flat plate collector and heat pipe evacuated tube collector, respectively. In order to get suitable water outlet temperature (60 °C), the SWH system is modelled with three collectors which are connected in series. Here, the outlet temperature of the second and subsequent collectors will be more and not the same as the first, because its inlet temperature is the outlet temperature of the first, and the water collects more and more energy along its way.

Cold water ($T_1$ = $T_{fi}$ = 22.5 °C) which have the same temperature with water entering the storage tank will be pumped to the inlet of the first collector where the sun radiation falls and energy is contained and trapped, thus heating the water contained in the tubes. The water heated (outlet) from the first collector ($T_2$) will be inlet to the second collector, where it collects more energy, which then increases the temperature of the water to ($T_3$). Finally, the water outlet from the second collectors will pass through the third collector where it is again heated to a higher temperature ($T_4$ = $T_{fo}$).

The rate of thermal energy of the tubular collector available will be carried away by the fluid flowing through the tube under steady-state conditions. This can be calculated using the energy balance on the fluid volume as follows:

$$Q_u = \dot{m}\, C_p\left(T_{fo} - T_{fi}\right) \tag{1}$$

The collector efficiency is defined as the ratio of the actual useful energy gain over a specific period of time to the incident solar energy over the same period, and it can be computed by the following equations:

$$\eta_{collector} = \frac{Q_u}{A_p\, I} \tag{2}$$

$$\eta_{1^{st}\,collector} = \frac{\dot{m}\, C_p(T_2 - T_{fi})}{I\, A_{C1}} \tag{3}$$

$$\eta_{2^{nd}\,collector} = \frac{\dot{m}\, C_p(T_3 - T_2)}{I\, A_{C2}} \tag{4}$$

$$\eta_{3^{rd}\,collector} = \frac{\dot{m}\, C_p (T_{fo} - T_3)}{I\, A_{C3}} \tag{5}$$

$$\eta_{overall\ collectors} = \frac{\dot{m}\, C_p (T_{fo} - T_{fi})}{I\, A_C} \tag{6}$$

The energy absorbed by the collector and output to the collector loop with heating losses is calculated as follows:

$$P = I_{dir}\, \eta_o\, f_{IAM} + \; f_{IAM_d}\; I_d\, \eta_o\, k_o (T_{Cm} - T_a)\, k_q (T_{Cm} - T_a)^2 \tag{7}$$

with $I_{dir}$ = Part of solar irradiation striking a tilted surface

$I_d$ = Diffuse solar irradiation striking a tilted surface

$T_{Cm}$ = Average temperature in the collector

$T_a$ = Air temperature

$f_{IAM}$ = Incident angle modifier

After deduction of optical losses, a part of the absorbed radiation is lost through heat transfer and radiation to the environment.

Orientation angle is set as face to south and no tracking device was used. According to Adama city water supply corporation [40], the temperature of water supplied for Adama is between 21 ºC and 24 ºC, so average temperature of 22.5 ºC was chosen as the water inlet temperature. Table 3 shows the characteristics of both collectors.

Table 3. Collector design parameters

| **Parameter** | **for ETC** | **for FPC** |
|---|---|---|
| Type | OPC 15 | KSC-AE/ 200/ S |
| Gross area of collector | 2.13 $m^2$ | 1.94 $m^2$ |
| Active area of collector | 1.7 $m^2$ | 1.7 $m^2$ |
| Length of collector | 1.25 m | 0.99 m |
| Width of collector | 1.7 m | 1.97 m |
| Number of collectors | 3 | 3 |
| Total active area of collector | 5.1 $m^2$ | 5.1 $m^2$ |
| Specific heat capacity of collector | 12413 $Ws/m^2$ K | 12059 $Ws/m^2$ K |
| Linear heat transfer coefficient | 1.02 $W/m^2$ K | 3.89 $W/m^2$ K |

| | | |
|---|---|---|
| Height of collector | 0.1 m | 0.1 m |
| Surface azimuth angle | 0 | 0° |
| Collector inclination | 20° | 20° |
| Water inlet temperature | 22.5 °C | 22.5 °C |

**3.5.2 Storage tank**

As in all hot water systems, the storage tank's task is to balance peak demand and charging power in supplying hot water by compensating for time differences between solar energy supply and hot water requirements. Dual coil indirect hot water tank is applied for the storage tanks modelling of both systems from the T*SOL® component library.

Since it's a closed loop solar water heating system, the storage tank will feature a heat exchanger at the bottom. Hence, heat absorbed by the water in the solar collectors is then transferred to the water in the cylinder through a heat exchanger. This takes place where, the cold water intake is always in the lowest storage tank layer and the heat transfer fluid (water coming out of the collector) does not come into direct contact with the water being heated. Finally, hot water is generally drawn from the highest layer of the storage tank.

Assuming a fully mixed storage scenario the energy stored ($Q_{st}$) in the tank is expressed as:

$$Q_{st} = \dot{m}\, C_p\left(T_{tank\ out} - T_{fi}\right) \quad (8)$$

The capacity of the storage tank should be large enough to cover for at least one day. For domestic hot water (DHW) storage, the tank should hold the average daily consumption (in *l*) for that residency. Using the previously mentioned average volume of 75 *l* per person per day [33], a five-person family will require a 375 *l* storage tank (5×75 l = 375 *l*), but to accommodate for guests or other unexpected personnel in the house, the tank is sized with a 20% allowance resulting a 450 *l* storage tank. The exterior of a storage tank would be insulated to retain heat and reduce losses. Specifications of the storage tank are given in Table 4.

Table 4. Hot water storage tank properties

| Parameter | Value |
|---|---|
| Type | Dual coil indirect hot water tank |
| Volume | 450 $l$ |
| Height | 1.35 m |
| Number of tanks | 1 |
| Insulation material | Mineral wool |
| Thickness of tank insulation | 0.1m |
| Thermal conductivity of insulation | 0.045 W/m K |

The SWH system efficiency is defined as follows:

$$SWH\ system\ efficiency = \frac{Energy\ output\ from\ the\ SWH\ system}{Irradiation\ on\ to\ the\ collector} \quad (9)$$

### 3.5.3 Pump

A Standard single speed pump is used to circulate water from the storage tank in the solar collectors. The pump is switched on and off by the temperature difference between the solar tank and the standby tank. The pump's input energy fluctuates between 3 to 6 kWh depending on the fluid volume flowrate fluid inlet temperature and other changing parameters. Gary [43], suggested possible operational flow rate of HTFs to be in the range of 40 to 250 l/h.

### 3.5.4 Pipe and insulation

Pipes of the solar system must be fitted with thermal insulation so that thermal dissipation from the pipes does not deteriorate a total efficiency of the solar system. Heated water from the collector passes through a pipe connected to the hot water storage tank. From there, cold water move down the pipes into the solar collector where it was being heated, again. In addition to this, there will be a pipe where the hot water gets transferred from the storage tank in to the building.

The single length of piping and the thermal conductivity coefficient for insulation is subdivided and entered for inside, outside, and between the collectors. Gary [43] recommended the pipe diameter and length of the pipe to be around 0.02 meters and more 10 meters, respectively. The distinction influences the calculation of piping losses. Mineral wool is commonly used as an insulation throughout a house in pipes, sidewalls, attics, floors, crawl spaces ceilings and basements [44]. Compared with normal pipe insulation materials, mineral wool has low thermal conductivity and maximum service temperature so, mineral wool is an ideal choice for insulation material. It is recommended to have the thickness of the insulation to approximate the nominal diameter of the pipe [39] thus, the insulation thickness will also be 0.02 meter. Some specifications of the pipe are given in Table 5.

Table 5. Specification of pipe and insulation

| Parameter | Value |
|---|---|
| Pipe length (Inside the building) | 7 m |
| Pipe length (Outside) | 4 m |
| Diameter of pipe | 0.02 m |
| Insulation type | Mineral wool |
| Insulation thickness | 0.02 m |
| Thermal conductivity of insulation | 0.045 W/m K |

### 3.5.5 Controller

The controller monitors the operational state of the solar system and ensures the most efficient use of the energy irradiated. This control principle compares the temperatures at the absorber and in the storage tank. If the absorber temperature is at a level above that of the storage tank, the circulation pump in the collector loop is switched on by the controller. The irradiation energy converted to heat in the absorber system is transported to the storage tank, whose temperature increases. When the temperature of the storage tank is equal to that of the absorber, no more energy can be supplied to the storage tank and the pump is switched off.

## 3.6 Simulation parameters of examined SWH systems

Simulation of two SWH systems is performed for two collectors, ETC and FPC of the same size and system design parameters. Though, the temperature requirement for domestic applications is known to be at 49 °C [45], the desired DHW temperature is set to be 60 °C, because the hot water storage regulation, AS1056 [41]. The thermal analysis will be performed for four different operating variables which includes weather conditions, volume flow rate, collector inclination angle as well as storage tank size. The system operating parameters and their range of variation is given in Table 6.

Table 6. Simulation parameters and their range of variation.

| **Variables** | **Simulation parameters** |
|---|---|
| Solar radiation and ambient temperature (weather conditions) | Hourly, daily and monthly |
| Volume flow rate | 80 *l*/h, 120 *l*/h, and 160 *l*/h |
| Inclination angle of collector | 10°, 20°, 30° and 40° |
| Storage tank size | 360 *l*, 450 *l* and 540 *l* |

## 3.7 Methodology

The steps used to assess the Performance of the two collectors based on the performance in this thesis were

i. Determining the incident solar irradiation level on the plane of the collector
ii. Estimating the daily hot water heating requirement of the consumer
iii. Sizing the solar water heating (SWH) system
iv. Analyzing the system's thermal performance through annual simulation using the T*SOL® simulation programme for solar thermal heating systems.
v. Record, organize and present the results in a meaningful way to discuss afterwards.

# CHAPTER FOUR

# Results and discussion

## 4.1 Validation of T*SOL simulation software

The validation focuses on the comparison between the the simulation software and the experimental results for FPC. The experimental results has been done by Farzad and Emad [46], for flat plate collector. The experiments were conducted at the solar energy research center of Islamic Azad University, South Tehran branch in an open loop system equipped with electrical heater for the pre-heating of fluid, circulation pump for flow rate regulation, and flat plate collector as specified in Table 7. The output from the simulation software (T*SOL) has been run according to same configuration and parameters done in experimental work by them. Since they provided no information about the ambient air velocity used in their experimental facility, it is assumed as 3 m/s.

Table 7. Design condition for flat plate collector

| Parameters | Value |
|---|---|
| Absorber area | 1.6 $m^2$ |
| Working fluid | Water |
| Optical efficiency | 76% |
| Inlet water temperature | 300 K |
| Emissivity of absorber plate | 0.92 |
| Thickness of the back insulation | 50 mm |
| Thickness of absorber plate | 0.75 mm |
| Thermal conductivity of the absorber plate | 237 W/m K |
| Thermal conductivity of the insulation | 0.04 W/m K |
| Inner diameter of pipes | 13 mm |
| Collector tilt | 40° |
| Adhesive resistance | Negligible |
| Thermal conductivity of water | 0.608 W/m K |
| Specific heat capacity of water | 4180 J/kg K |
| Dynamic viscosity of water | 0.0004 kg/m s |

| | |
|---|---|
| Thermal conductivity of insulator | 0.045 W/m K |
| Thermal conductivity of absorber plate | 384 W/m K |
| Mass flow rate | 0.04 kg/s |

According to the results given in Table 8, there is a very good agreement between the experimental data [46], and the simulation predicted data of efficiency, absorber plate temperature and overall heat loss coefficient of the collector. In all the cases, the simulation software yields a result that is closely less or greater than the predicted values. The absolute errors of T*SOL for the collector efficiency, absorber plate temperature and overall heat loss coefficient for FPC system are 4.95%, 0.39% and 16.8%, respectively. This shows that, the simulation software (T*SOL) can be used to analyse any SWH problem since it gives almost same values as compared to the experimentation done in Farzad and Emad's research paper.

Table 8. The comparison between the simulation and experimental results

| **Output parameters** | **T*SOL** | **Experiment [46]** | **Difference** |
|---|---|---|---|
| Collector efficiency (%) | 48 | 50.5 | -4.95 |
| Absorber plate temperature (K) | 306.3 | 307.5 | -0.39 |
| Overall heat loss coefficient ($W/m^2 K$) | 3.4 | 2.91 | +16.8 |

## 4.2 Comparative analysis on effects of operating parameters on the SWHs

The collector's comparative thermal analysis is performed with four operating variables namely, weather conditions, volume flow rate, collector orientation angle as well as system size, to study how each variable's parameters affect the tank and collector outlet temperature, energy collected and accumulated in the tank and collector, efficiency and solar fraction of the system.

### 4.2.1 Effect of weather conditions

Fig. 8 shows trend of the changing energy collected by the collector that has been observed for all twelve months for a fluid circulating at 120 *l*/h, where the purple line represents ETC and the blue one is for FPC. For ETC, the maximum daily energy collected at the collector was found during November to be between 18 and 21.7 kWh/day and a minimum energy was collected in July to be between 6.1 and 18.2 kWh/day. FPC's maximum daily energy collected at the collector was found again in November ranging between 13 and 19.1 kWh/day while the minimum energy was collected in June to be between 3.9 and 15.5 kWh/day. Thus, November and July represented the highest and lowest monthly mean energy collected for both collectors, respectively where, for ETC, the highest mean energy collected is 20.1 kWh/day (in November) and the lower is 16.7 kWh/day (July), and for FPC, the highest mean energy collected is 17 kWh and the lower is 13.9 kWh/day. The total energy collected by the collector during November is 603.6 kWh/month and 510.3 kWh/month for ETC and FPC, respectively. Averagely, ETC has collected an energy that is 15.4% and 16.8% more higher than that of FPC for June and November, respectively. It is apparent that during winter months, solar intensity can get low by which the systems won't be performing at their maximum energy level, whereas during summer its value gets higher. These shows, as solar radiation increases, so does the radiation absorbed by the absorber plate and the evacuated tubes, thus the energy gained by the solar collector increases. However, when the solar radiation increases the desired increase in the efficiency of solar collector may not be obtained due to the limit of absorption capacity of heat transfer fluids and increase of thermal losses.

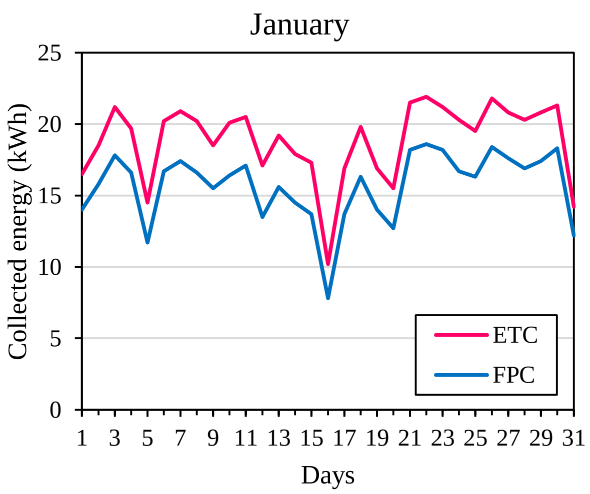


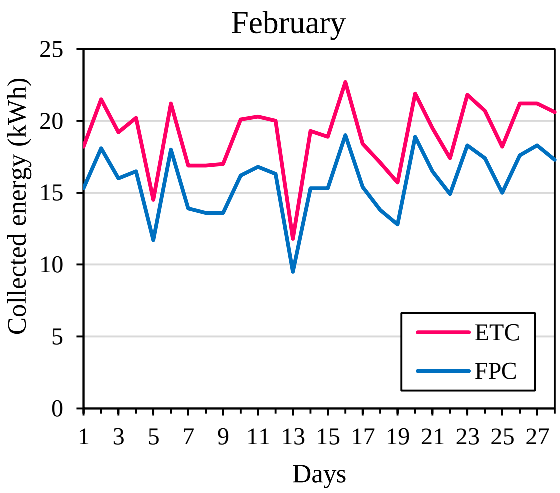

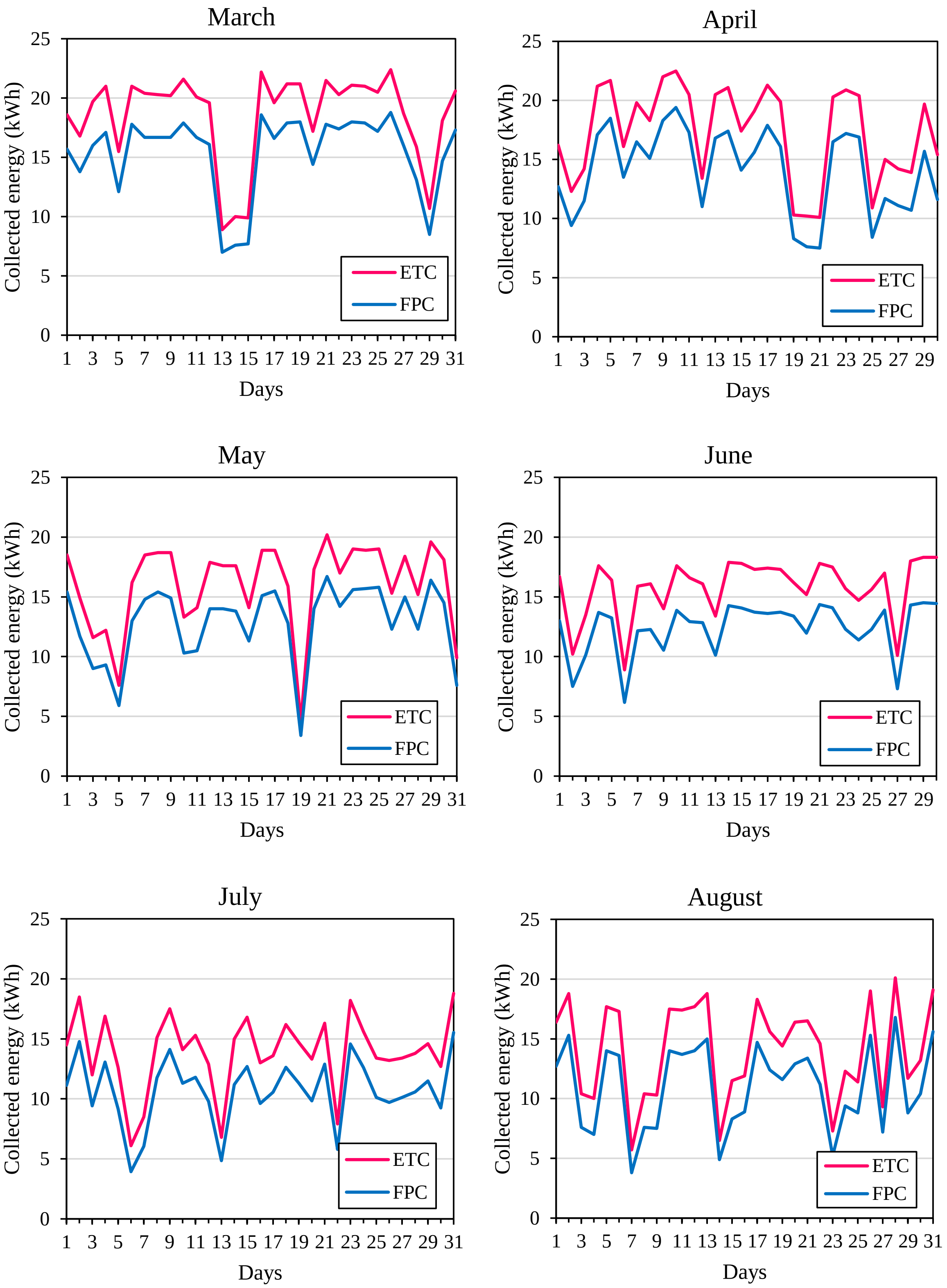
March
April
May
June
July
August
Collected energy (kWh)
Days
ETC
FPC
0
5
10
15
20
25
1 3 5 7 9 11 13 15 17 19 21 23 25 27 29 31
1 3 5 7 9 11 13 15 17 19 21 23 25 27 29

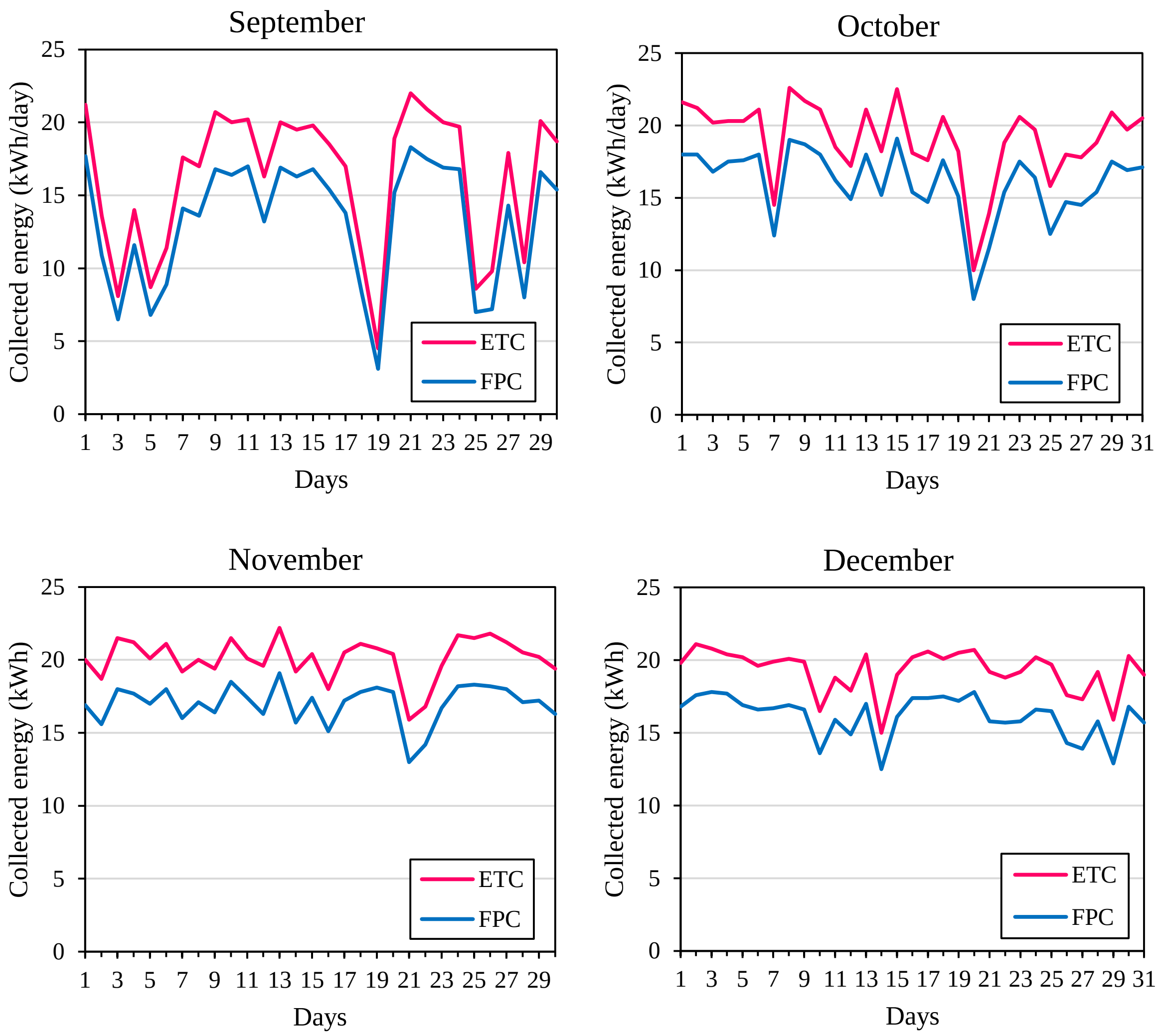


Figure 8. Daily energy collected by the collector for each month

Fig. 9 shows the annual solar fraction of both SWH systems, since to demonstrate the actual effect of weather conditions on the solar fraction in a DHW system, it is necessary to analyse the entire year of operation of such systems, including the periods characterized by less favourable weather conditions (lower solar energy inputs and lower ambient air temperatures). As it is shown in the figure, the solar fraction of both systems closely follow the profile of the global solar irradiation showing their dependency on the available solar energy. The monthly solar fraction of ETC's system varied between 64% in August and 80% in November meanwhile, FPC's monthly solar fraction varied between 47.5% (in August) and 64.6% (in October). The lowest solar fraction was found during August ('Nehase' for Ethiopian calendar) at a solar irradiation of 152 kWh/m$^2$/month. It should be noted that this period includes only small portion of the annual insolation in the city of Adama, thus, a low solar fraction was expected. The highest solar fractions of both systems were recorded during March and

November (‘Megabit’ and ‘Hidar’ in Ethiopian calendar) at a solar irradiation of 191 kWh/m$^2$. The higher energy collection in this period is primarily associated with the greater average solar energy elevation in spring months. As more favourable atmospheric conditions prevailed, higher values of radiation intensity will be observed. The aftermath is, temperature of the collector will be increasing and in turn a faster rise of temperature of water in the tank will be observed. Hence, the system will be more capable of fulfilling the hot water demand. The mean annual solar fraction in the case of ETC was 73.7%, while in the case of FPC it was 57.1%. Therefore, using ETC over FPC in this case improved the annual solar fraction by 22.5%.

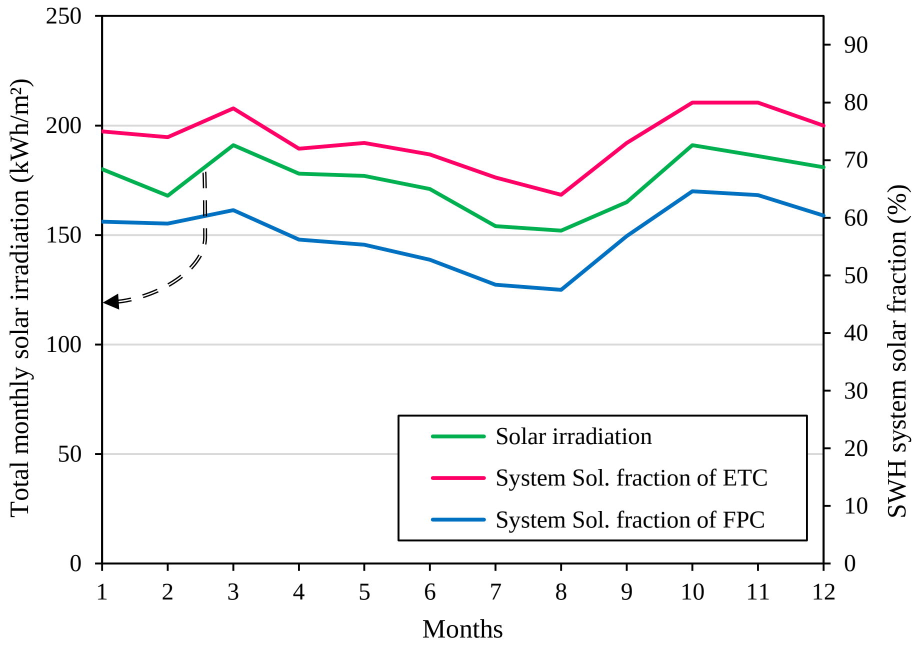


Figure 9. SWH System solar fraction at different solar irradiation throughout a year

Fig. 10 demonstrates each storage tank’s hourly variations of outlet temperature of water for each month of a year. For a given day, the difference between the highest and lowest tank outlet temperature of each collector varies with each month. Out of all months, the highest tank outlet temperature of the water occurred in November, and the outlet temperature at this month varied between 43 and 87 °C for ETC, and 33.6 and 71.2 °C for FPC at 9:00 AM and 12:00 PM, respectively. Once again, the highest mean tank outlet water temperature was found in November to be 58 °C for ETC and 45.4 °C for FPC. These higher tank outlet temperatures are a result of a higher solar radiation intensity and higher ambient air temperatures that exist during this month (November). During this period, a large temperature difference will be developed between the air and the tubes which leads to a higher heat transfer rate from the air to the fluid, increasing the temperature of the fluid that is transferred to the storage tank. August gave the lowest mean tank outlet water temperatures of 38.2 and 33.8 °C for ETC and FPC, respectively. The lower outlet temperature were found during Winter months, because average ambient air temperature and the solar radiation intensity of this season are significantly lower than of the other warm seasons. This results in a significant drop in the average daily temperatures of the water in the storage tank.

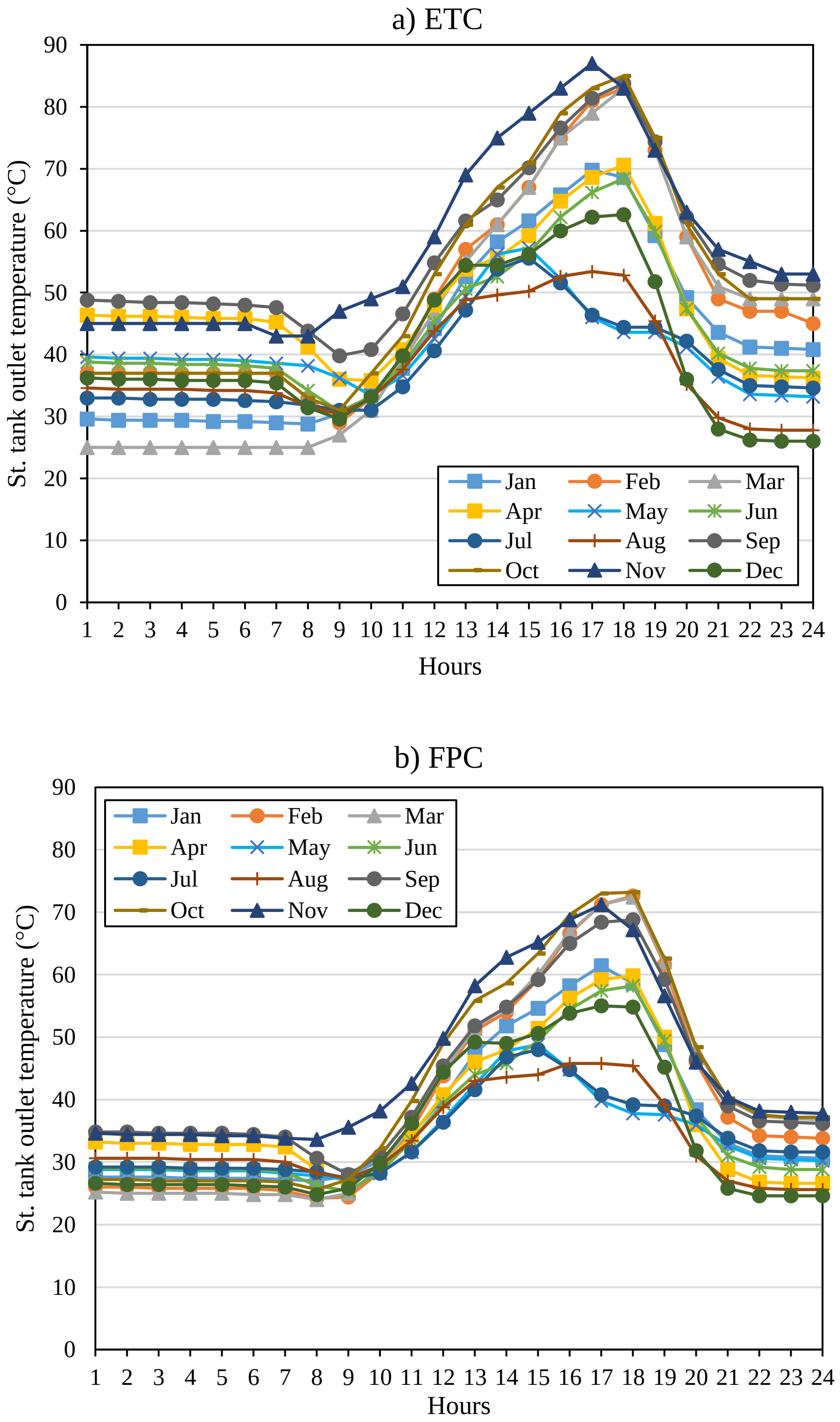


Figure 10. Hourly tank outlet temperature of ETC and FPC SWH system for each month

Fig. 11 shows the amount of energy collected by the two collectors throughout a day and it obviously shows, higher solar radiation will result in higher amount of energy collected by the collector that reaches its peak during noon and then decreases with the solar intensity. The ambient temperature causes significant variation in the net heat absorption capacity at higher solar intensity and the effect is relatively insignificant at lower solar intensity. For the total solar intensity throughout a day, ETC has collected an energy that is 18.6% higher than that of FPC. At noon, the daily solar irradiation on the active areas of the collectors can get as high as 4.19 kW and the energy accumulated in the collectors would reach 2.71 kWh/day for ETC and 2.26 kWh/day for FPC. Correspondingly, ETC and FPC collected 59.1% and 48.04% of the solar intensity throughout the day. A higher solar intensity yields a higher rate of heat absorption by the working fluid. This is due to the fact that, when the ambient temperature increase with the solar intensity, the heat transfer rate to the fluid increases. In addition to that, with the rise of solar intensity, there is a significant increment in radiative heat transfer between the outer glass and the inner glass tube (for ETC) and between the glass and absorber plate for (FPC), hence there is an increase in net heat energy absorbed by the working fluid.

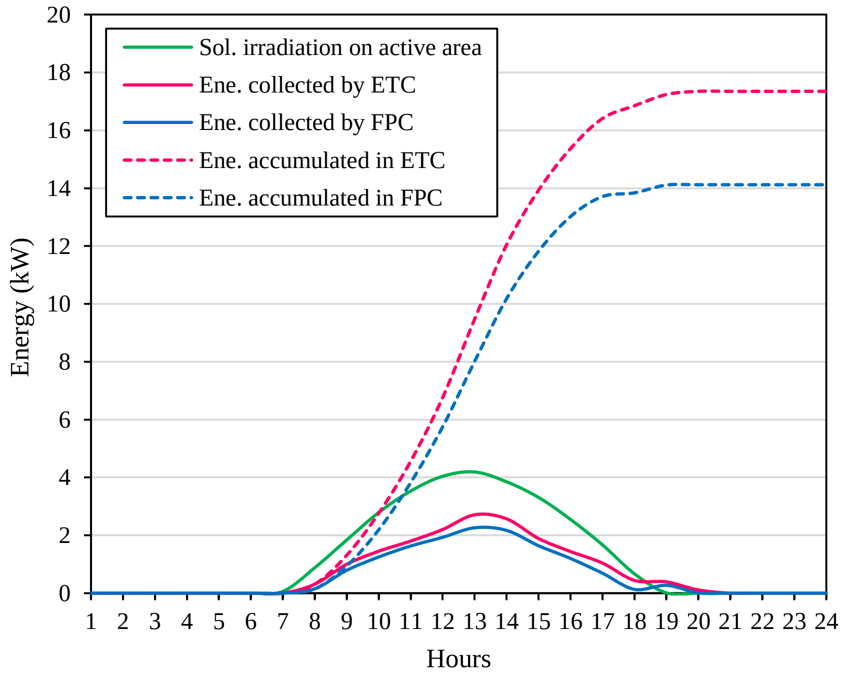


Figure 11. Influence of solar intensity on energy collected and accumulated by the collectors in a day

### 4.2.2 Effect of volume flow rate

Fig. 12 compares the time wise variation of storage tank outlet temperature of water with different volume flow rates. Here, the analysis is done for volume flow rates of 80, 120 and160 *l*/h. For a particular day in April, at the highest flow rate (160 *l*/h), the tank outlet temperature of water can reach up to 74 °C and 62.5 °C for ETC and FPC, respectively. It is certain that increasing the amount of flow rate of the working fluid raises the tank outlet temperatures in each situation. For example for ETC, the mean tank outlet temperature has been improved by 14.06% as the volume flow rate is increased from 80 to 120 *l*/h, and by 6.36% as the volume flow rate is again increased from 120 to 160 *l*/h, also for FPC the mean tank output temperature of the fluid has been improved by 12.7% and 6.21% for the same respective flow rate boosts. The reason behind this is, though, at lower flow rates there is a longer period of contact between the working fluid and tube (heat pipe wall for ETC), it takes a while for the water to reach the storage tank, so in the meantime, it will lose much of its heat to the surrounding before it reaches the tank. But, at higher flow rate the fluid can quickly reach the tank without losing much heat and transfer it through the heat exchanger, hence there is an increase in the tank outlet temperature. The differences between the mean daily tank outlet temperatures of the two systems has been obtained indicating ETC's tank outlet temperature to be higher than FPC's by 20.3%, 21.5% and 21.6% for a volume flow rate of 80, 120 and 160 *l*/h, respectively.

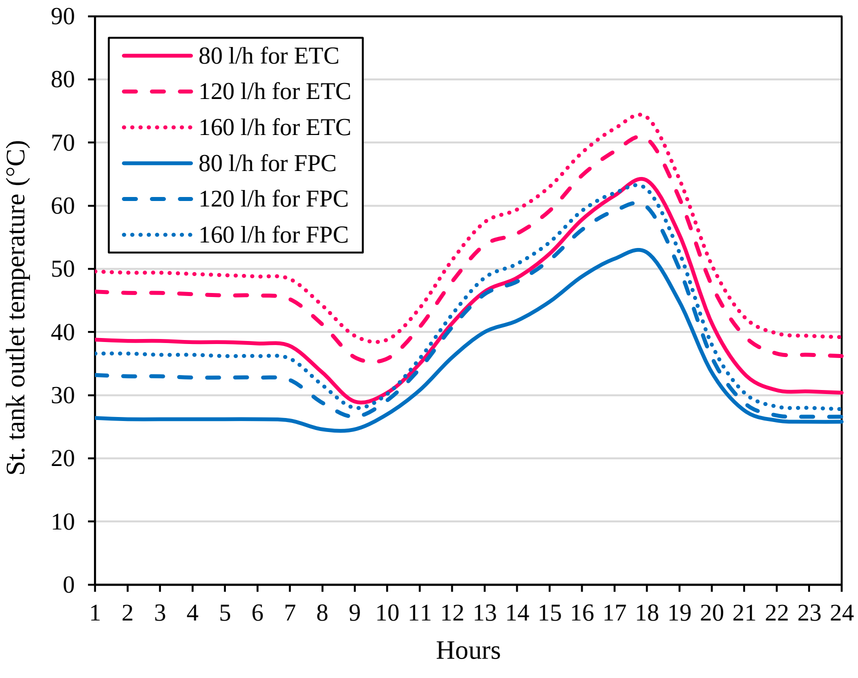


Figure 12. Storage tank outlet temperatures ETC and FPC for different flow rates on a typical day

Fig. 13 displays the variation of SWH system efficiency for different volume flow rates of the fluid as a function of the parameter $T_i$-$T_a/I_T$. This is a usual parameter for expressing the thermal efficiency of solar collectors. In comparative simulation of these two collectors, the highest SWH system efficiencies were achieved at a volume flow rate of 160 *l*/h for both ETC and FPC. This phenomenon is due to the decrease in the overall thermal loss of the collector at higher flow rates. Although the efficiency obtained at a flow rate of 80 l/h is low, it is a more preferable situation for the winter season. Nevertheless, a volume flow rate of 160 *l*/h emerges as a preferred value throughout a year, because it is at this volume flow rate that the highest efficiency of 59% and 50% could be achieved for ETC and FPC, respectively, at inlet water temperature of 22.5 °C. ETC's system efficiency has shown to be higher than FPC's by 28.6%, 21% and 18.21% for a volume flow rate of 80, 120 and 160 *l*/h, respectively. Increasing the inlet water temperature also reduces the efficiency of the system by 3 to 8% based on water inlet temperature. Both ETC and FPC presented a significant drop in the efficiency values at lower flow rates, since at lower fluid flow rates, the collector temperature rises and more heat will be lost out through the glazing and absorber plate (for ETC), then this heat loss reduces the heat output of the collector. However, high volume flow rates at low inlet water temperatures and solar radiation values can be disadvantageous since it can cause the outlet temperature to be lower, which is the basic purpose of SWHs.

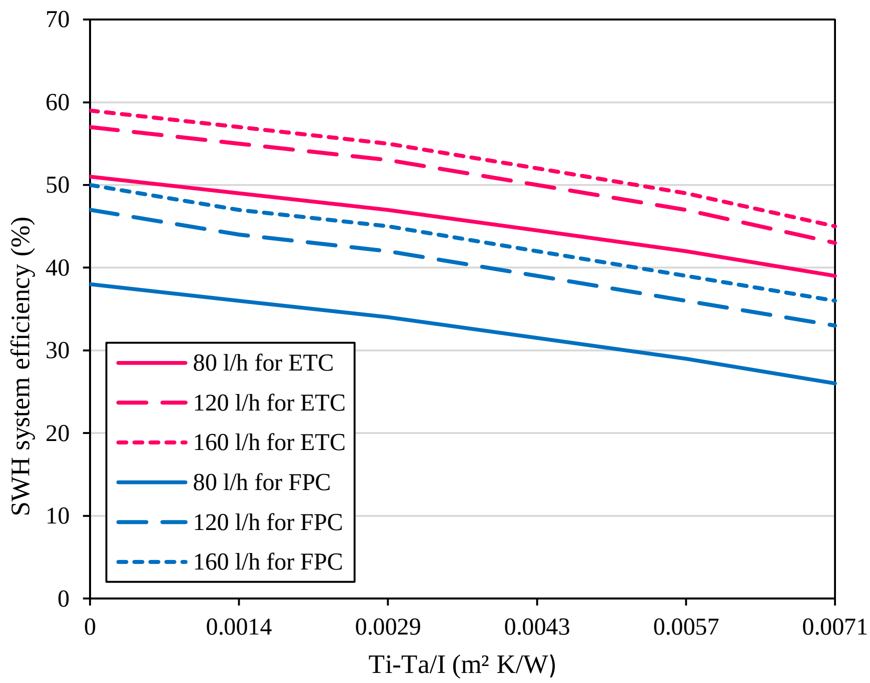


Figure 13. Variation of SWH system efficiency with different flow rates

Fig. 14 demonstrates the actual effect of fluid flow rates on the solar fraction in a SWH system. The solar fraction of both SWH systems increased with increasing volume flow rates. ETC's mean monthly solar fractions are 66.1%, 73.7% and 75.2% for 80, 120 and 160 *l*/h, respectively, while in case of FPC, the corresponding solar fractions becomes 47.5%, 57.1% and 60.1%. The monthly lowest and highest solar fraction of ETC's system exist during August and November, respectively, and lies between 57.8% and 72.2% for 80 *l*/h, between 64% and 80% for 120 *l*/h and between 65% and 82% for 160 *l*/h. In contrast, FPC's monthly lowest and highest solar fraction values existed for the same months as ETC's (August and November, respectively) and varied between 39.8% and 53.6% for 80 *l*/h, between 47.5% and 64.6% for 120 *l*/h and between 49.6% and 68.1% for 160 *l*/h. Hence, the lowest solar fraction was recorded at a flowrate of 80 *l*/h, in which it did not exceed 55% in both cases systems. The highest system solar fraction of both collectors were found at a flow rate of 160 *l*/h, and for ETC, its value amounted to 82%, while, it is 68.1% in the case of FPC. Therefore, the use of high volume flow rates increased the energy absorption and usage of water in the storage tank, thus improved the annual solar fraction the systems averagely by 12.1% and 20.9% for ETC and FPC, respectively, when the flow rate is increased from 80 to 160 *l*/h.

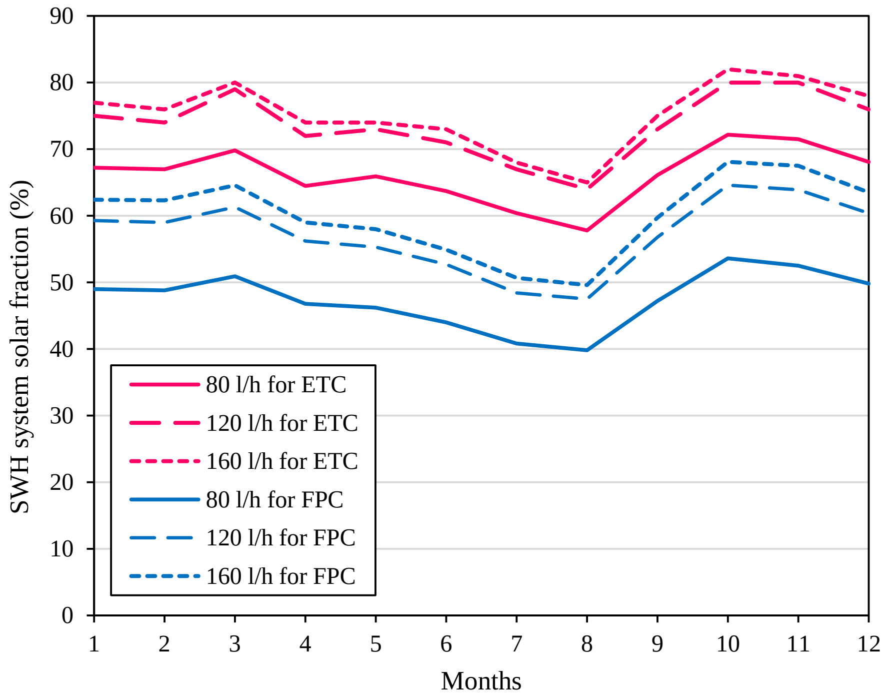


Figure 14. Variation of solar fraction with fluid flow rate throughout a year

### 4.2.3 Effect of collector inclination

Fig. 15 shows the effect of varying collector inclination on the solar fraction of a SWH system which circulates fluid at 120 *l*/h. Solar fraction is defined as the amount of energy provided by the solar collector (system) divided by the total energy required by the system. For both collectors, it's evident from the graph that at an inclination angle of 10°, relatively consistent solar fraction can be achieved than any other inclination angles, since a collector at this inclination has a better chance of picking up the solar radiation from wide range of angles. For ETC, the variation of inclination angle; 10, 20, 30 and 40° gives a respective annual solar fraction of 74, 72.8, 70.6 and 66.4% respectively, and for FPC, at these inclination angles, the annual solar fraction will be 57.1, 56.6, 54.7 and 51.4%, respectively. This indicates, for Adama, a city located at 8.33° N, a stationary flat plate and evacuated collector would give a better performance if it is installed at low inclination angle, preferably 10°. The reason for this being, at this angle the collector is oriented in such a way that it will minimize the angle of incidence and maximize the transmittance of the glass cover and absorptance of the absorber plate hence, absorbs the maximum amount of solar radiation for most days of a year. As seen from the figures, the variation of inclination angle from 10 to 20° is not largely critical to the performance of flat plate and evacuated tube collectors since the annual solar fraction of both systems is almost the same, decreasing only by 1%. Beyond 20°, with each 10° increase in collector inclination, the annual solar fraction of both collectors reduces roughly by 5%. Based on the results, for each inclination angle, the annual solar fraction of ETC is higher than FPC, thus it can meet the heating load requirement more efficiently than FPC. It is clear from the figures that, a unique optimum tilt angle exists for each month of a year that corresponds to the maximum point of each curve.

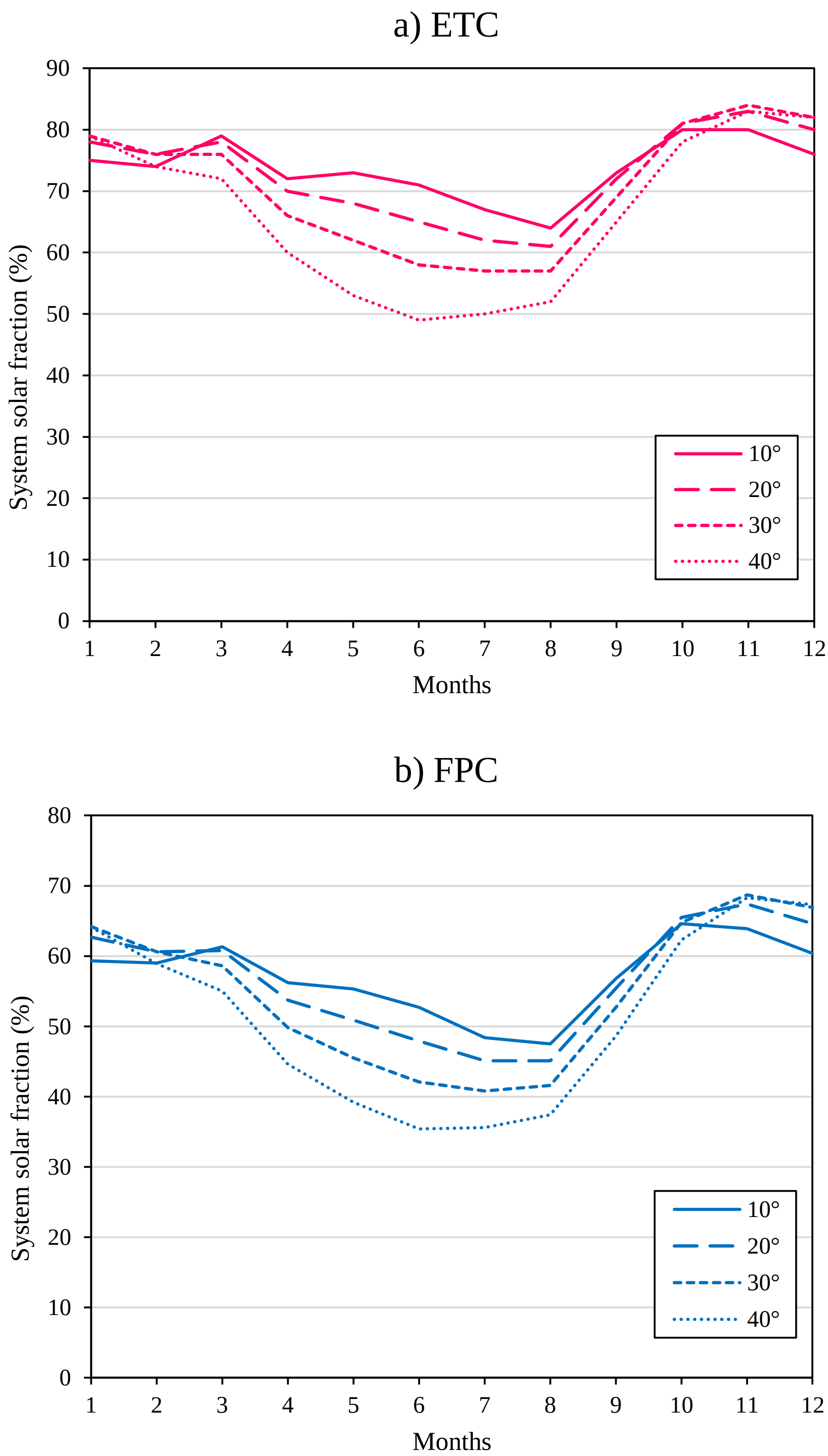


Figure 15. Monthly solar fraction for ETC and FPC SWH systems at different inclinations

The optimum tilt angle of different months have been discussed in earlier sections to determine the best inclination angles of each month, but for stationary solar collectors it will be necessary to figure out and decide a fixed angle which will be capable to extract the most out of the available solar radiation. Fig. 16 demonstrates the variation of collector outlet fluid temperature as a function of different tilt angle of solar collectors. ETC's mean hourly collector outlet temperature were 40 °C, 39.2 °C, 38 °C and 36.6 3 °C for 10, 20, 30, and 40°, respectively, while in case of FPC, the corresponding mean hourly collector outlet temperature became 36.2°C, 35.6 °C, 34.7 °C and 33.5 °C. The results show that in Adama, Ethiopia, the best performance for ETC and FPC occurs when the collector is tilted at angle around 10°. Therefore, the tilt angle of both collectors can be taken as 10°, since the highest hourly collector outlet temperature was found at this inclination angle to be 74.5 and 65 °C for ETC and FPC, respectively.

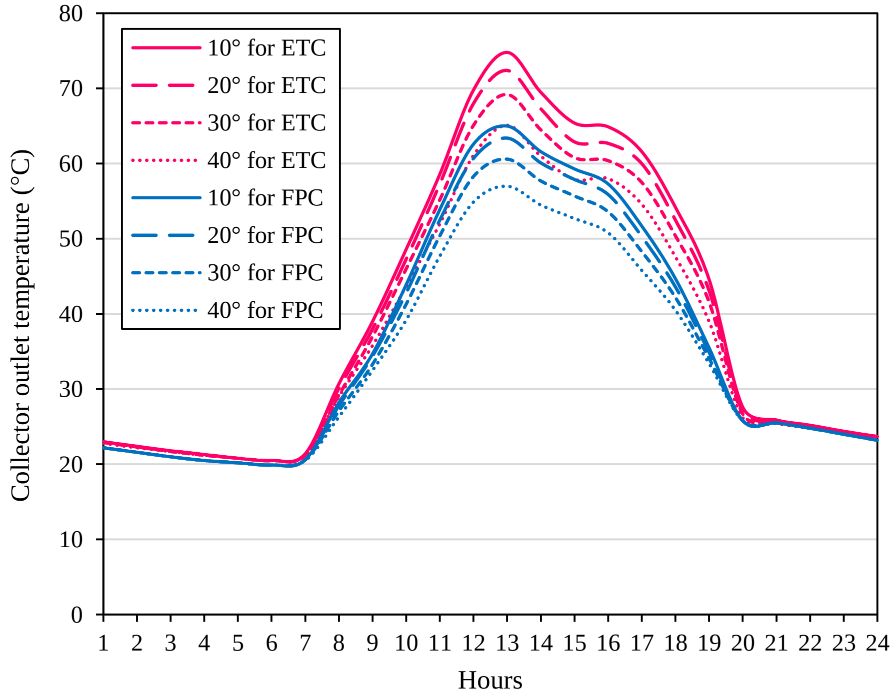


Figure 16. Variation of annual energy gain as a function of different tilt angles

The yearly useful energy collected from the ETC and FPC for four different collector inclination angles (10, 20, 30 and 40°) are shown in Fig. 17. The results showed the yearly useful energy accumulated for ETC at 10°, 20°, 30° and 40° is about 6332, 6285, 6100 and 5780 kWh/year, respectively and 5178, 5142, 4975 and 4683 kWh/year for FPC, so the corresponding yearly energy accumulated in ETC is around 0.7, 4 and 9% less than FPC for a full year. It is also observed that, the yearly useful energy accumulated in ETC is around 18% more than that of FPC for each inclination angle. The results showed that, more energy would be accumulated at lower inclination angles which is around the latitude of Adama city for both ETC and FPC.

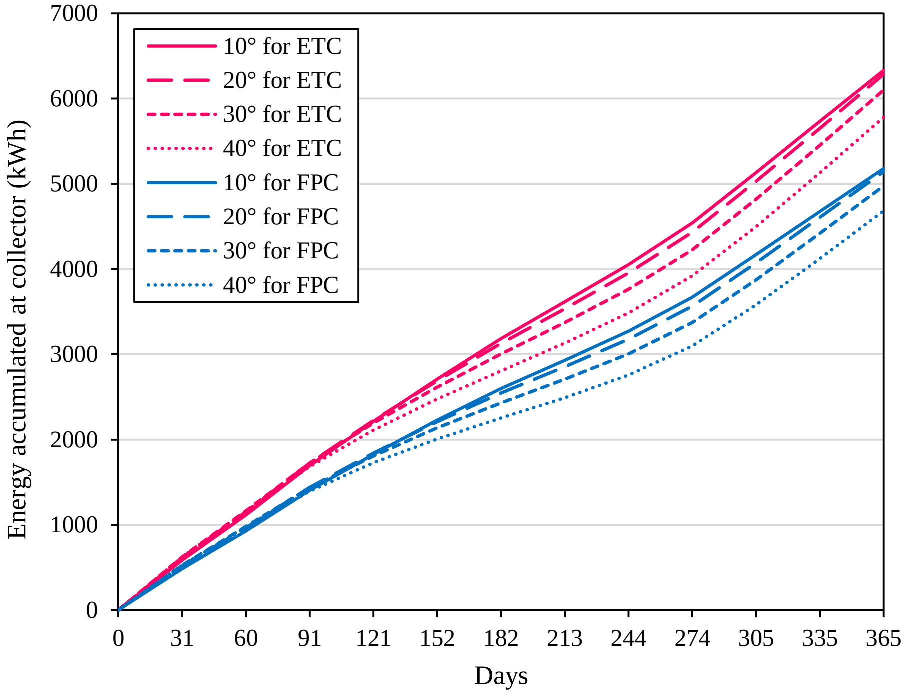


Figure 17. Energy accumulated at a collector for different inclinations throughout in a year

### 4.2.4 Effect of storage tank size

Size is one of the most important parameters of SWH systems because the total system size is associated with the demand for DHW and the type of heat source. The effect of storage tank size on the energy accumulated in the tank of both ETC and FPC SWH systems is shown in Fig. 18 for 360, 450 and 540 *l* tanks. ETC's energy accumulation in the tank increased with each day, and at the end of a year it reached 6074.1 kWh/year, 6266.3 kWh/year and 6390.5 kWh/year for 360, 450 and 540 *l*, respectively, whereas for FPC, at the end of a year the energy accumulation add up to 4836.6 kWh/year, 5127.93 kWh/year and 5335.43 kWh/year, for 360, 450 and 540 *l*, respectively. Overall, as the tank volume is increased from 360 to 450 and 540 *l*, the energy accumulated in the tank increased for ETC's system by 3.1 and 4.9% and for FPC's system by 5.69 and 9.34%, respectively.

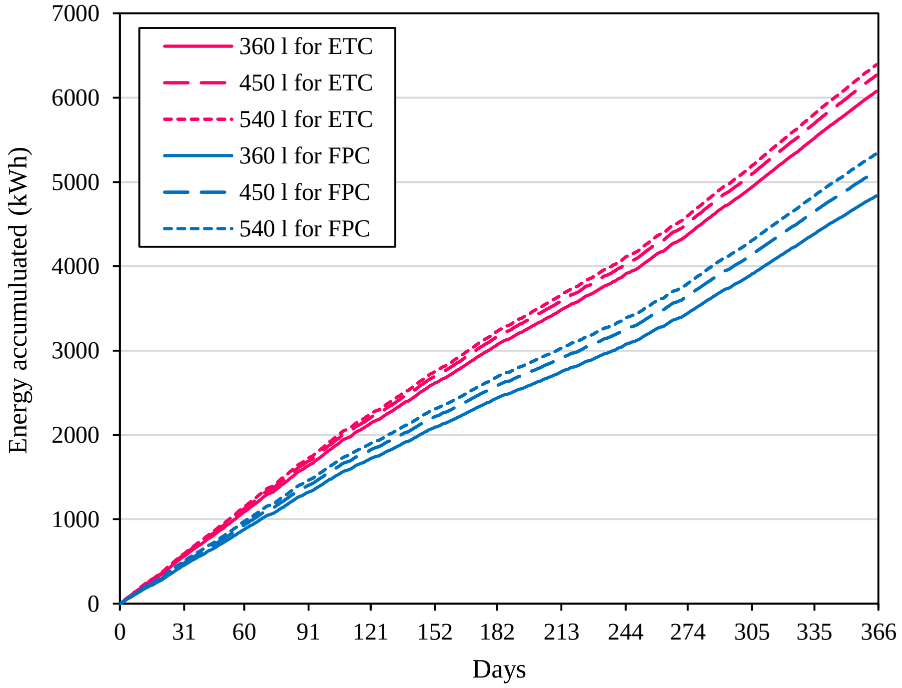


Figure 18. Energy accumulated at a storage tank of different sizes throughout a year

As it is shown in Fig. 19, the hourly storage tank outlet water temperatures of the three different storage tank sizes are determined for both systems. For a particular day, the maximum tank outlet temperature decreased as the tank size (volume) increased. By increasing the tank size from 360 *l* to 450 *l* then 540 *l*, the respective maximum attainable tank outlet temperature of water decreased from 75.2 °C to 70.6 °C and 68.2 °C for ETC and from 62.8 °C to 59.8 °C and 57.6 °C for FPC. However, the daily mean tank outlet temperature increased with the tank size and for ETC, the mean tank outlet temperature became 47.4, 48.1 and 48.9 °C for the 360, 450 and 540 *l*, respectively, and the corresponding tank outlet temperatures for FPC were, 36.2, 37.7 and 39.1 °C. Compared to using the 360 *l* tank, employing 450 *l* and 540 *l* correspondingly resulted the mean daily tank outlet temperature to be increased by 1.39% and 1.86% for ETC, and 3.87% and 3.66% for FPC. The increase in mean tank outlet temperature is in response to the tank increment which in turn increases the amount of incoming (collector outlet) hot water that can be stored in the tank, thus smaller tanks will have higher tank inlet temperatures. But, a larger tank size also increases the amount of inlet water that is fed to and stored in the tank, which then the low heat energy gets balanced with the tank inlet hot water, so it will ultimately give a relatively lower tank outlet temperature.

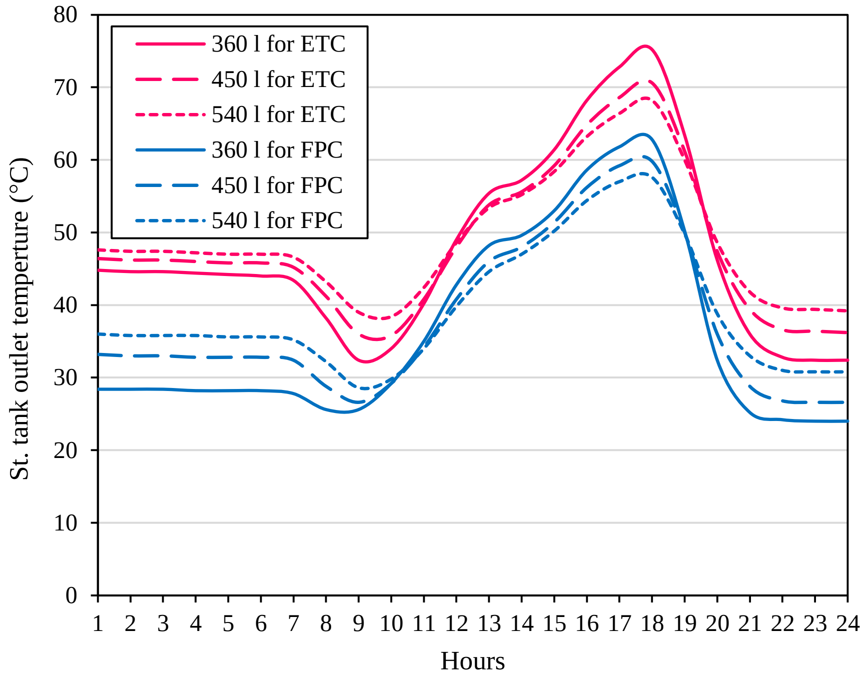


Figure 19. Variation of hourly tank outlet temperature with size

The effect of adopting a larger and smaller storage tanks on the solar fraction of the SWH system has been shown in Fig. 20. The system solar fraction for ETC's SWH system is 72%, 74% and 74.1%, for 360, 450 and 540 *l*, respectively and the system solar fraction for FPC's SWH system is 55.1%, 57.1% and 58.5%, for 360, 450 and 540 *l*, respectively. For ETC system with a 450 litre storage tank, increasing and decreasing the size of the tank by 90 litres (by one person with a safety factor) consequently reduced and improved the system solar fraction only by 2.2 and 0.54%. For FPC, with the same tank volume (450 *l*), increasing the size of the tank by 100 litres to 540 *l* improved the solar fraction by 3.5% while decreasing the volume by 100 litres to 360 *l* reduced the solar fraction only by 2.4%. Though it is known that the performance increases with the size of the overall system, the adoption of a larger storage tank in itself doesn't really change the annual solar fraction of both systems considerably. This indicates, the improvement of collector performance due to change in tank size is barely sufficient to compensate the increase in heat loss from the larger tank.

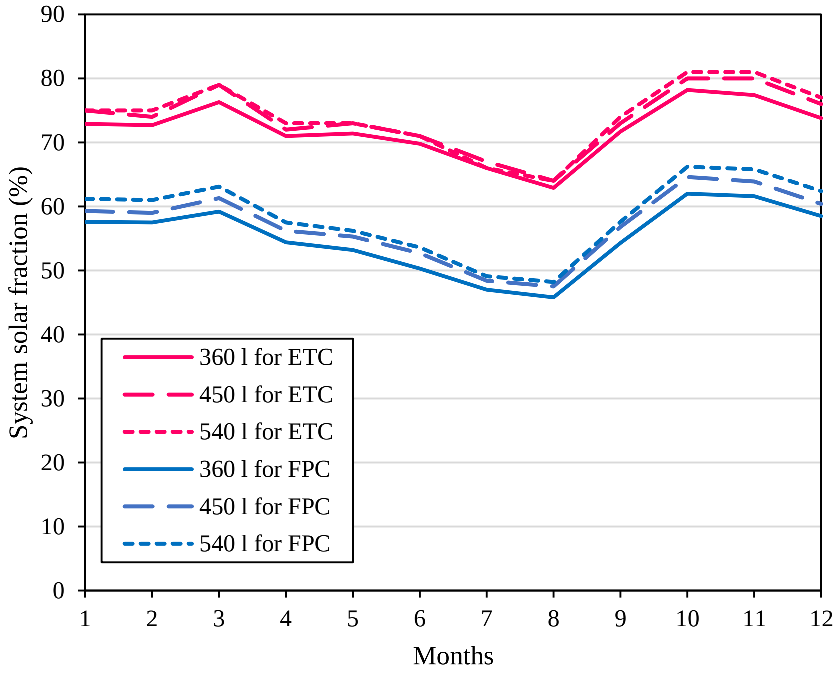


Figure 20. Variation of solar fraction a SWH system for different storage tank volumes

## 4.3 Collector, pipe and tank losses of the proposed SWH systems

FPCs have collector heat losses due to the temperature difference between the absorber and ambient air that results to convection and radiation losses. The convection losses are caused by the angle of inclination and the spacing between the glass cover and the absorber plate, while the radiation losses are caused by the exchange of heat between the absorber and the environment. For ETC, conductive and convective heat losses are greatly reduced because there is no air to conduct heat or to cause convective losses. But, there is some radiant heat loss (heat energy will move through a space from a warmer to a cooler surface, even across a vacuum). Fig. 21 shows monthly global solar irradiation on the collector and also the surface and optical loss of the collectors. The total monthly solar irradiation on the collector's active area varied between 761 kWh/month in July and 1030 kWh/month in November. The highest and lowest optical losses were also recorded in the months of November and July in which for ETC, it varied between 219 and 299 kWh/month while for FPC it's between 239 and 299 kWh/month. The surface loss of ETC varied between 52 and 59 kWh/month whereas FPC's varied between 134 and 165 kWh/month. Here, unlike the solar irradiation and optical loss, lowest values of the surface losses were recorded in August. The corresponding monthly average optical loss of ETC and FPC becomes 264.4 and 273.2 kWh/month, while the surface losses are 58 and 151.3 kWh/month. In general, the annual global solar irradiation on the collector's active area is 10962 kWh/year, from which a total of 3869 kWh/year and 5094 kWh/year were lost in the collectors of ETC and FPC, respectively. Averagely, 28.9 and 6.35% of ETC's collected solar radiation is allotted to the optical and surface losses respectively, while 29.9 and 16.6% of this energy is lost as optical and surface loss in FPC. Thus, optical losses are proved to be the main source of energy loss within a collector. During months of January to February and October to December the optical loss of ETC is greater than that of FPC's since the sunlight hitting the tubular solar collector is reflected with much more radiation than FPC's as only small part of beams gets on tube perpendicularly and the majority of the beam is reflected. During the remaining months, the optical loss of FPC is higher because, as the sunshine fall on the surface with an angle, the shade of sunlight increases and the quantity of the radiation getting through gaps between the tubes decreases.

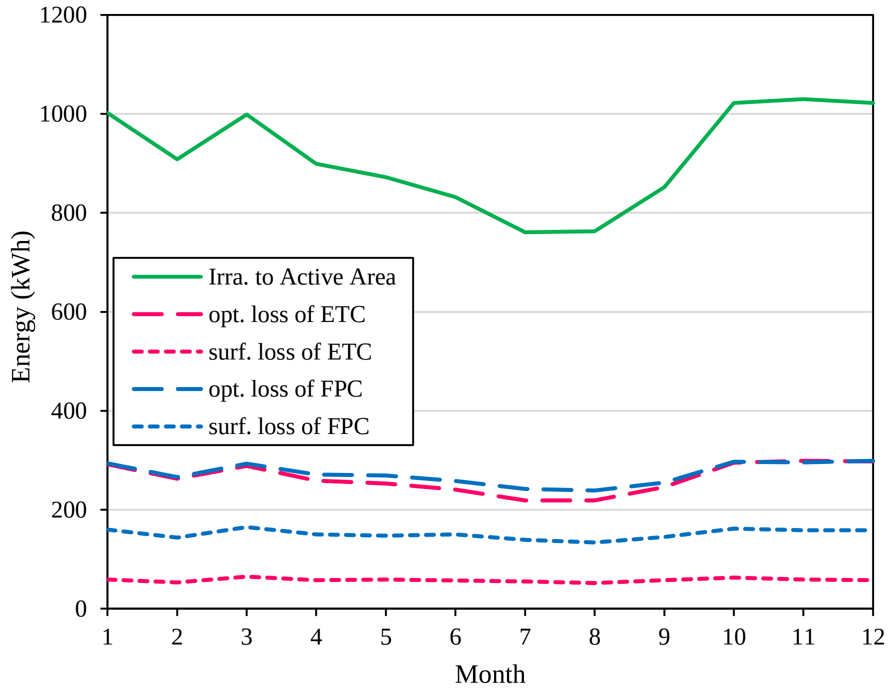


Figure 21. Average monthly optical and surface losses of ETC and FPC

Fig. 22 shows monthly energy losses of internal and external pipe which are used to interconnect the collector, tank and other components of the systems. The former represents a pipe installed inside the building while the latter is for a pipe outside a building. Pipe losses are due to temperature drop as the fluid flows between the collector outlet, the coil inlet to the storage tank and to the appliances. For an annual solar irradiation of 10962 kWh/year, a total of 7093 and 5868 kWh/year were delivered to the pipes of ETC and FPC, respectively. Monthly internal pipe loss of ETC varied between 36.7 and 51.7 kWh/month, whereas the external pipe loss varied between 17.7 and 20.9 kWh/month. FPC's monthly internal pipe loss varied between 28.3 and 41.7 kWh/month, while the external pipe loss varied between 12.6 and 14.9 kWh/month. Knowing high temperature seasons contribute to higher performance of the systems, this shows heat losses along the supply side of the solar circuit occurred especially at high collector outlet temperatures being transported through pipes. Annual external pipe loss of the ETC and FPC SWH systems were 233.4 and 168.5 kWh/year, respectively. Annual internal pipe loss of ETC and FPC systems were 527 and 423 kWh/year, respectively. The total annual supply pipe loss was 760.4 and 591.5 kWh/year for ETC and FPC, respectively. Overall, for both systems, around 4% of the collector's energy was lost by the external pipe and 12% of energy was lost by the internal pipe when delivered to the storage tank. The internal pipe loss was higher compared to the external one due to its large length. The supply pipe length should therefore be kept as short as possible and all joints insulated to reduce heat losses otherwise, it is necessary to place the storage tank inside the building on which the collectors are installed.

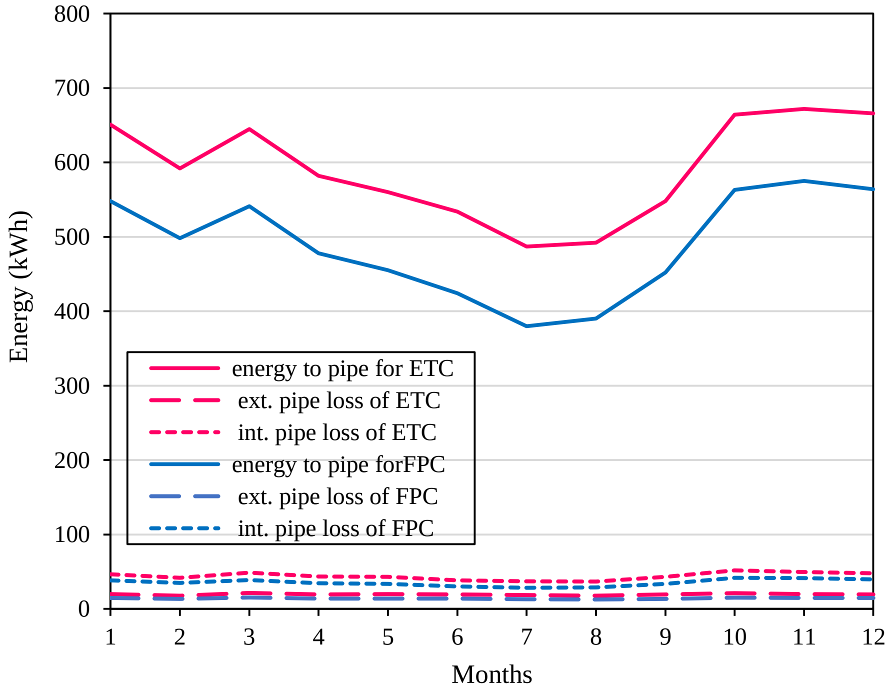


Figure 22. External and internal pipe losses of ETC and FPC SWH systems

Fig. 23 shows monthly energy losses of both ETC and FPC at the storage (hot water) tank. Annually, 6332.6 kWh/year and 5276.5 kWh/year of energy was delivered to the storage tank of ETC and FPC systems, respectively. The monthly storage tank loss of ETC varied from 23.8

to 29.9 kWh/month, and for FPC, it varied from 17.7 to 22.5 kWh/month. This shows regardless of the amount of energy transferred to it, the energy loss of the storage tank is somewhat consistent throughout a year. The mean monthly tank loss is found to be 27.8 kWh/month and 20.5 kWh/month and the annual tank loss is 309.4 and 242.2 kWh/year for ETC and FPC, respectively. Thus, the tank loss of ETC is 26.2% higher than that of FPC's. ETC system's tank loss is higher than FPC system's since it collects and stores more energy in the storage tank. Even though the storage tank is well insulated, thermal (heat) losses from the tank to the environment occur through the tank's wall, top and bottoms surfaces due to the high tank storage temperatures.

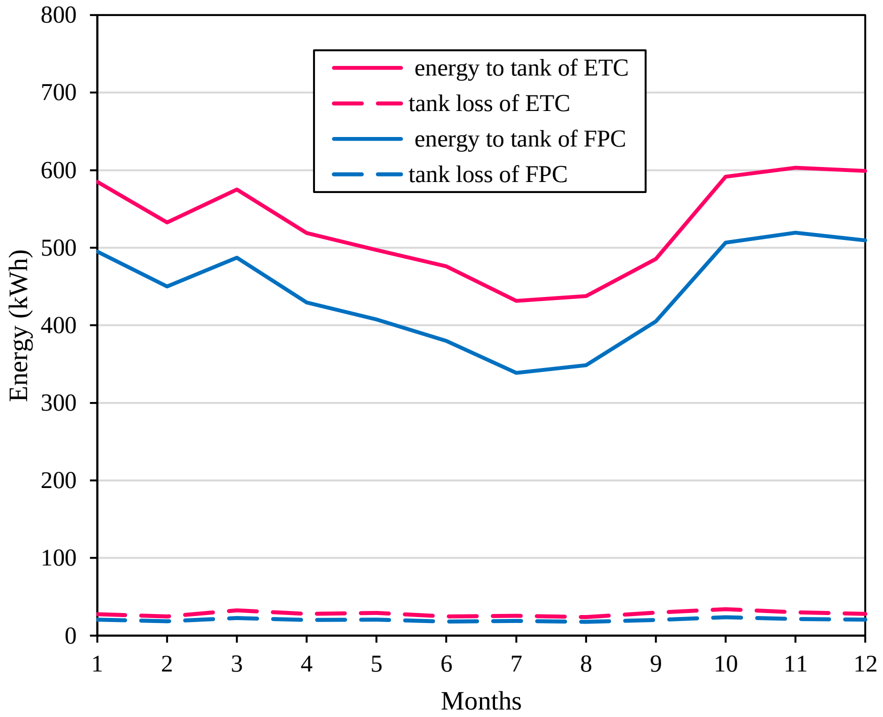


Figure 23. Energy collected and lost at the storage tank

# CHAPTER FIVE

# Conclusion and recommendation

## 5.1 Conclusion

In this study, an hourly, daily, monthly and seasonal year-round thermal performance analysis of a commonly used SWH systems with ETC and FPC was carried out by using T*SOL® Pro simulation programme. The software is used to mimic real life operation taking into consideration of the interaction between the collectors, storage tank and users. The analysis of the SWH system regarding the estimation of the daily heating load was based on domestic hot water demand. The influencing characteristics of the volume flow rate, weather conditions, collector inclination angle and the storage tank size were discussed in details.

The results from the study showed, that the system efficiency, solar fraction and tank outlet temperature increased with the volume flow rate due to the increase in the heat supplied to the fluid. Thus, it can be concluded that the collectors will be more efficient operating at relatively high flow rates such as 160 *l*/h, but there will only be a low collector outlet temperature rise. If the flow rate is decreased all the way to 80 *l*/h, collector outlet temperature rises. However, more heat will be lost to the surrounding through the glazing, tubes and absorber plate, and these losses reduce the heat output of the collectors.

The monthly total solar radiation, incident on the collector surface have a maximum value during October to December and minimum value during July to August. Sunny seasons and warmer climates are usually associated with higher water temperatures since, higher solar radiation will result in higher amount of energy collected by the collector. Despite the promising effects of the use of SWHs, this study showed that during the colder season it was difficult to obtain satisfying water temperatures in the storage tank in the cases of both systems. Water inlet temperature can be associated with weather condition and at higher inlet temperature, the useful energy collected will decrease.

A yearly average fixed tilt angle is utilized for both DHW systems in Adama, and a relatively maximum solar fraction is found at low inclination angles, preferably 10°. Only March and September gave a more or less consistence optimum inclination angle which is again, around 10°. The optimum tilt angle escalates during the winter months and reaches its maximum value in December while it drop down during the winter season.

The collectible solar radiation energy shows a small sensitivity storage tank size variation, and the performance of ETC's water heating system was found to be even less sensitive to it than FPC. It was showed that, a higher collector area doesn't corresponds to maximum system solar fraction but to maximum tank outlet temperature.

The system lost the sun's collected energy at various points of the system such as the collector, pipe and storage tank. ETCs lose their heat mainly by radiation and FPC losses their heat due to convection and radiation losses. Losses within a collector are mainly attributed to the optical loss while the pipe loss is mostly for the internal piping. Out of the three components (collector, pipe and storage tank), the system lost most of its heat in the collector.

## 5.2 Recommendation

Based on the results from this study the following recommendations can be made

1. During the colder season (July - August), less heat will be collected by the solar collector, so it was impossible to obtain satisfying water temperatures in the storage tank in the cases of both systems. Thus, to substantially increase the temperature of the water in the tank along with avoiding legionella growth, it's better to use an auxiliary heater in addition to the house's solar heating system.
2. The performance of SWH systems can be studied using simulation softwares like T*SOL®, which can be used to design and simulate solar thermal systems with hot water supply, swimming pool heating, process heat and large-scale systems.

# References


[1]. Soteris A. Kalogirou, (2004). Solar thermal collectors and applications, Progress in Energy and Combustion Science 30 231–295.

[2]. Piotr Feli´nski, Robert Sekret, (2017). Effect of PCM application inside an evacuated tube collector on the thermal performance of a domestic hot water system, Energy and Buildings 152, 558–567.

[3]. Fikremariam Teshome, (2014). Assessment of Solar Energy Resources in Ethiopia Modeling solar radiation and GIS-based multi-criteria analysis.

[4]. Melessaw Shanko, (2009). Ethiopia's Solar Energy Market,Target Market Analysis.

[5]. Yan, C., Wang, S., Ma, Z.,Shi, W., (2015). A simplified method for optimal design of solar water heating systems based on life-cycle energy analysis. Renewable Energy 74, 271–278.

[6]. Myeong Jin Ko, (2015). Analysis and Optimization Design of a Solar Water Heating System Based on Life Cycle Cost Using a Genetic Algorithm, Energies.

[7]. Kalogirou S, (2003). The potential of solar industrial process heat applications, Application Energy, 37–61.

[8]. Yirga Belay, Gelana Amente, Girma Goro, (2016). Estimation of Solar Panel Orientation with Different Tilt Angles at Haramaya University, Research.

[9]. Soteris A. Kalogirou, Sotirios Karellas, Viorel Badescu, Konstantinos Braimakis, (2016). Exergy analysis on solar thermal systems: A better understanding of their sustainability, Renewable Energy 85, 1328-1333.

[10]. Soteris A. Kalogirou, Sotirios Karellas, Konstantinos Braimakis, Camelia Stanciu, Viorel Badescu, (2016). Exergy analysis of solar thermal collectors and processes, Progress in Energy and Combustion Science 56, 106–137.

[11]. Adissu Bekele, Demiss Alemu & Manish Mishra, (2013). Large-scale solar water heating systems analysis in Ethiopia: a case study, International Journal of Sustainable Energy 32:4, 207-228.

[12]. Kamal Anoune, Mohsine Bouya, Abdellatif Ben Abdellah, Abdelali Astito, (2017). Optimizing and Controlling the Productivity of a Flat Plate Collector by Using an Electronic System, Energy Procedia, 107, 180 – 187.

[13]. Alper Mete Genc, Mehmet Akif Ezan, Alpaslan Turgut, (2018). Thermal performance of a nanofluid-based flat plate solar collector: A transient numerical study, Applied Thermal Engineering 130, 395–407.

[14]. Sassan M and Alibakhsh K, (2014). Comparing the Performance of Flat Plate Collector and Evacuated Tube Collector for Building and Industrial Usage in Hot and Cold Climate in Iran with TRNSYS Software.

[15]. Weiqiang Konga, Zhifeng Wang, Jianhua Fan, Bengt Perers, Ziqian Chen, Simon Furbo, Elsa Andersen, (2012). Investigation of thermal performance of flat plate and evacuated tubular solar collectors according to a new dynamic test method, Energy Procedia 30, 152–161.

[16]. Himangshu Bhowmik, Ruhul Amin, (2017). Efficiency improvement of flat plate solar collector using reflector, Energy Reports 3, 119–123.

[17]. Ayompe, L., Duffy, A., McCormack, S., McKeever, M., Conlon, M., (2011). Comparative Field Performance Study of Flat Plate and Heat Pipe Evacuated Tube Collectors (ETCs) for Domestic Water Heating Systems in a Temperate Climate. Energy, Vol. 36, Issue 5, pp. 3370-3378.

[18]. Chandraprabu V., Sankaranarayanan G., Iniyan S. and Suresh S., (2013). Performance of CuO/Water Nanofluid as Outer Fluid in the Tube in Tube Condensing Unit of Air Conditioner: Experimental Study, Journal of Nanofluids 2, 213–220.

[19]. Siva Kumar S., Mohan Kumar K., Sanjeev Kumar S. R, (2017). Design of Evacuated Tube Solar Collector with Heat Pipe, Materials Today: Proceedings 4, 12641–12646.

[20]. Budihardjo I, Morrison G, Behnia M., Development of TRNSYS models for predicting the performance of water-in-glass evacuated tube solar water heaters in Australia, Proceedings of ANZSES Annual Conference Melbourne 256.

[21]. Adel A. Ghoneim, Hany M. Shabana, Mohamed S. Shaaban and Adel M. Mohammedein, (2016). Performance Analysis of Evacuated Tube Collector in Hot Climate, European International Journal of Science and Technology 5, ISSN: 2304-9693.

[22]. Xianhua Nie, Li Zhao, Shuai Deng, Xueyin Lin, (2017). Experimental study on thermal performance of U-type evacuated glass tubular solar collector with low inlet temperature, Solar Energy 150, 192–201.

[23]. Zhihua Zhou, Junwei Liu, Xin Huang, (2018). Tianjin Key Laboratory of Indoor Air Environmental Quality Control, Key Laboratory of Efficient Utilization of Low and Medium Grade Energy, Advances in Engineering Research, volume 163.

[24]. Piotr Feli´nski, Robert Sekret, (2017). Effect of a low cost parabolic reflector on the charging efficiency of an evacuated tube collector/storage system with a PCM, Solar Energy 144, 758–766.

[25]. Ajinkya Sable, (2017). Experimental and economic analysis of concrete absorber collector solar water heater with use of dimpled tube, Resource-Efficient Technologies 3, 483–490.

[26]. Guillermo Martínez-Rodríguez, Amanda L. Fuentes-Silva, Martín Pic_on-Núnez, (2017). Solar thermal networks operating with evacuated-tube collectors, Chemical Engineering Transactions 52, 859-864.

[27]. Rigardt Alfred Maarten COetze, Aggrey Mwesigyw, Zhonglie Huan, (2016). Optimal slope angle selection of an evacuated tube collector for domestic solar water heating, Energy in southern Africa 28, 1.

[28]. Kiran Naik B., Varshney A., Muthukumar P., Somayaji C., (2016). Modelling and Performance Analysis of U Type Evacuated Tube Solar Collector Using Different Working Fluids, Energy Procedia 90, 227–237.

[29]. Dimitri Loginov, Teet-Andrus Koiv, Mikk Maivel, Kalev Kalda, (2015). Thermal performance of evacuated tube and flat plate solar collectors in Nordic climate conditions, Mechanical Engineering and Technology 6, 81-91.

[30]. Duffie, J.A., Beckman, W.A., (2013). Solar Engineering of the Thermal Processes, John Wiley and Sons, New York.

[31]. Kaunda. C.S., (2005). Computer Aided Design and Economic Analysis of a Solar Water Heating System, Unpublished MSc thesis, Department of Mechanical Engineering, KNUST, Ghana.

[32]. https://www.cerbos.ee/img/cms/paikesekute/kuidas-valida-paikesekollektor-paikesepaneel-eng

[33]. https://www.cerbos.ee/img/cms/paikesekute/kuidas-valida-paikesekollektor-paikesepaneel-eng

[34]. Mclaughlin R.K., Mclean R.C., Bonthron W.J., (1981). Heating Services Design, Butterworth & Company Ltd, London.

[35]. ASHRAE, (1995). Handbook of Heating and Ventilation of Air Conditioning Applications, Atlanta.

[36]. Roger Taylor, (2006). Solar thermal technology and applications, NREL 7.

[37]. Tiwari, Arvind, G.N Tiwari, Shyam (2016). Energy Systems in Electrical Engineering, Handbook of Solar Energy Theory, Analysis and Applications, ISSN 2199-8590.

[38]. U.S.A Department of Defence, Solar heating of buildings and domestic hot water.

[39]. Valentin G., (2005). T*SOL, A windows TM programme for the Design and Simulation of Solar Thermal Systems, Berlin-Germany.

[40]. Derara Chalchisa, Moa Megersa and Abebe Beyene, (2017). Assessment of the quality of drinking water in storage tanks and its implication on the safety of urban water supply in developing countries, Environ Syst Res 6, 12.

[41]. AS1056.1, (1991). Standards Australia, Storage Water Heaters – General Requirements.

[42]. Ethiopia Rural Socioeconomic Survey (ERSS), (2013). Central Statistical Agency & the World Bank Survey Report.

[43]. Gary reysa, (2015), Determining collector flow rate, Build it solar, https://www.builditsolar.com/References/ColflowRate.htm,

[44]. Soltau, H., (1992). Testing the Thermal Performance of Uncovered Solar Collectors, Solar Energy 49, Issue 4, 263-272.

[45]. U.S. Consumer Product Safety Commission. Shower Systems May Present Scalding Risk When Not Properly Installed And Adjusted, Office of Information and Public Affairs.

[46]. Farzad Jafarkazemi and Emad Ahmadifard, (2013). Energetic and exergetic evaluation of flat plate solar collectors, Renewable Energy 56, 55-63.

# Appendix A

## Climate data for Adama, Ethiopia from *Meteosyn* tool

Table 9. Monthly climate data collected for a year

| **Months** | **Ta [°C]** | **G. Rad [kWh/m²]** | **v [m/s]** |
|---|---|---|---|
| Jan | 25.3 | 180 | 1.61 |
| Feb | 25.4 | 168 | 1.51 |
| Mar | 25.1 | 191 | 1.5 |
| Apr | 24.7 | 178 | 1.89 |
| May | 24.1 | 177 | 2.2 |
| Jun | 22.3 | 171 | 2.19 |
| Jul | 22.1 | 154 | 2.4 |
| Aug | 22.8 | 152 | 2.3 |
| Sep | 24.4 | 165 | 2.4 |
| Oct | 26.8 | 191 | 2.49 |
| Nov | 27 | 186 | 2.4 |
| Dec | 26.1 | 181 | 1.8 |

Table 10. Daily climate data collected for each month

| **January** | | | |
|---|---|---|---|
| **Days** | **Ta [°C]** | **G. Rad [kWh/m²]** | **v [m/s]** |
| 1 | 29.3 | 4.93 | 1.36 |
| 2 | 27.1 | 5.51 | 1.15 |
| 3 | 27.6 | 6.46 | 1.74 |
| 4 | 25.8 | 6.07 | 0.97 |
| 5 | 25.2 | 4.5 | 1.52 |
| 6 | 24.9 | 6.11 | 1.53 |
| 7 | 25 | 6.32 | 0.85 |
| 8 | 24.2 | 6.15 | 1.96 |
| 9 | 23.6 | 5.63 | 1.47 |
| 10 | 24 | 6.27 | 3.02 |
| 11 | 24.7 | 6.29 | 2.26 |
| 12 | 20.4 | 5.42 | 1.06 |
| 13 | 22.5 | 5.93 | 1.5 |
| 14 | 22.9 | 5.55 | 0.76 |
| 15 | 21.5 | 5.45 | 2.65 |
| 16 | 23.2 | 3.26 | 0.82 |
| 17 | 24.5 | 5.3 | 1.78 |
| 18 | 25.4 | 6.03 | 2.31 |
| 19 | 26.4 | 5.2 | 2.28 |
| 20 | 26.1 | 4.8 | 1.64 |

| | | | |
|---|---|---|---|
| 21 | 27.3 | 6.48 | 3.17 |
| 22 | 27.8 | 6.62 | 1.46 |
| 23 | 25.9 | 6.44 | 0.49 |
| 24 | 23.8 | 6.47 | 0.83 |
| 25 | 24.3 | 6.15 | 0.73 |
| 26 | 26.9 | 6.66 | 1.77 |
| 27 | 26.7 | 6.37 | 3.32 |
| 28 | 25.6 | 6.24 | 1.53 |
| 29 | 26.2 | 6.35 | 1.32 |
| 30 | 26.6 | 6.47 | 1.32 |
| 31 | 28.5 | 4.58 | 1.13 |

| **February** | | | |
|---|---|---|---|
| **Days** | **Ta [°C]** | **G. Rad [kWh/m²]** | **v [m/s]** |
| 1 | 28.1 | 5.58 | 1.71 |
| 2 | 27.2 | 6.56 | 1.72 |
| 3 | 26 | 5.95 | 0.7 |
| 4 | 22.9 | 6.36 | 1.36 |
| 5 | 24.9 | 4.6 | 1.66 |
| 6 | 24.5 | 6.56 | 1.25 |
| 7 | 25.4 | 5.44 | 0.79 |
| 8 | 23.2 | 5.39 | 1.23 |
| 9 | 22.6 | 5.41 | 1.57 |
| 10 | 23.7 | 6.28 | 1.06 |
| 11 | 24.2 | 6.37 | 2.08 |
| 12 | 23.5 | 6.32 | 1.47 |
| 13 | 25.8 | 3.67 | 1.54 |
| 14 | 21.2 | 6.3 | 2.07 |
| 15 | 21.9 | 6.08 | 3.95 |
| 16 | 24.7 | 7.14 | 1.54 |
| 17 | 26.2 | 5.83 | 2.45 |
| 18 | 24 | 5.44 | 1.01 |
| 19 | 25.7 | 4.97 | 0.93 |
| 20 | 26.9 | 6.78 | 1.44 |
| 21 | 28.7 | 6.28 | 1.47 |
| 22 | 29.2 | 5.5 | 1.63 |
| 23 | 26.6 | 6.86 | 1.4 |
| 24 | 26.7 | 6.53 | 1.52 |
| 25 | 26.4 | 5.76 | 1.06 |
| 26 | 25.2 | 6.73 | 1.15 |
| 27 | 27 | 6.64 | 1.41 |
| 28 | 27.6 | 6.73 | 1 |

| March | | | |
| --- | --- | --- | --- |
| **Days** | **Ta [°C]** | **G. Rad [kWh/m²]** | **v [m/s]** |
| 1 | 25.7 | 6.16 | 1.09 |
| 2 | 25.4 | 5.46 | 2.02 |
| 3 | 23.4 | 6.4 | 1.31 |
| 4 | 22.7 | 6.86 | 1.01 |
| 5 | 23 | 5.14 | 1.07 |
| 6 | 24.2 | 6.77 | 1.91 |
| 7 | 23.8 | 6.93 | 2.23 |
| 8 | 20.8 | 6.99 | 1.77 |
| 9 | 21.6 | 6.84 | 1.45 |
| 10 | 22.4 | 7.23 | 1.53 |
| 11 | 24 | 6.67 | 0.25 |
| 12 | 23.6 | 6.52 | 1.08 |
| 13 | 24.2 | 2.93 | 1.57 |
| 14 | 24.7 | 3.34 | 1.45 |
| 15 | 25.7 | 3.21 | 1.54 |
| 16 | 26.4 | 7.24 | 1.64 |
| 17 | 28.7 | 6.35 | 0.96 |
| 18 | 28.1 | 6.91 | 0.98 |
| 19 | 27.2 | 6.99 | 1.52 |
| 20 | 24.6 | 5.68 | 1.09 |
| 21 | 25 | 7.34 | 2.62 |
| 22 | 26.7 | 6.91 | 1.05 |
| 23 | 26.2 | 7.14 | 1.8 |
| 24 | 26.3 | 7.07 | 1.96 |
| 25 | 25.9 | 6.85 | 1.34 |
| 26 | 25.2 | 7.56 | 2.24 |
| 27 | 26.9 | 6.18 | 1.22 |
| 28 | 26.5 | 5.48 | 2.34 |
| 29 | 25.5 | 3.53 | 1.12 |
| 30 | 26 | 5.93 | 2.14 |
| 31 | 27.4 | 6.79 | 1.14 |

| April | | | |
| --- | --- | --- | --- |
| **Days** | **Ta [°C]** | **G. Rad [kWh/m²]** | **v [m/s]** |
| 1 | 23.1 | 5.55 | 2.23 |
| 2 | 23.4 | 4.11 | 2.66 |
| 3 | 24.2 | 4.7 | 0.57 |
| 4 | 24.4 | 7.3 | 0.91 |
| 5 | 27.1 | 7.5 | 1.6 |
| 6 | 26.5 | 5.47 | 1.08 |

| | | | |
|---|---|---|---|
| 7 | 27.5 | 6.58 | 2.68 |
| 8 | 26.8 | 6.1 | 1.75 |
| 9 | 26.1 | 7.44 | 2.69 |
| 10 | 27.9 | 7.6 | 2.65 |
| 11 | 28.4 | 7.34 | 0.53 |
| 12 | 25.6 | 4.78 | 2.63 |
| 13 | 25.2 | 6.94 | 1.86 |
| 14 | 24.8 | 7.23 | 3.55 |
| 15 | 25.2 | 5.87 | 3.64 |
| 16 | 25 | 6.47 | 1.03 |
| 17 | 23.9 | 7.28 | 0.61 |
| 18 | 23.9 | 7.17 | 1.1 |
| 19 | 22.3 | 3.76 | 1.62 |
| 20 | 23.4 | 3.4 | 1.9 |
| 21 | 23 | 3.38 | 1.99 |
| 22 | 24.1 | 6.99 | 1.17 |
| 23 | 24.5 | 7.27 | 3.73 |
| 24 | 22.9 | 7.09 | 1.78 |
| 25 | 24.6 | 3.79 | 1.08 |
| 26 | 24.4 | 5.05 | 3.03 |
| 27 | 24.8 | 4.8 | 1.97 |
| 28 | 23.5 | 4.69 | 1.83 |
| 29 | 21.9 | 6.91 | 0.96 |
| 30 | 21.4 | 5.4 | 1.73 |

| **May** | | | |
|---|---|---|---|
| **Days** | **Ta [°C]** | **G. Rad [kWh/m²]** | **v [m/s]** |
| 1 | 24.3 | 6.35 | 2.62 |
| 2 | 25 | 5.34 | 1.07 |
| 3 | 24.8 | 3.94 | 0.5 |
| 4 | 24.6 | 4.18 | 1.6 |
| 5 | 25.5 | 2.49 | 0.45 |
| 6 | 25.9 | 5.51 | 1.8 |
| 7 | 24 | 6.47 | 1.8 |
| 8 | 23 | 6.57 | 2.13 |
| 9 | 22.3 | 6.99 | 2.07 |
| 10 | 21.9 | 4.81 | 1.49 |
| 11 | 23.1 | 4.86 | 2.56 |
| 12 | 20.7 | 6.43 | 1.28 |
| 13 | 22.5 | 6.23 | 2.95 |
| 14 | 21.3 | 6.31 | 4 |
| 15 | 23.9 | 4.77 | 4.02 |
| 16 | 23.4 | 6.93 | 5.52 |
| 17 | 23.2 | 6.99 | 2.25 |

| | | | |
|---|---|---|---|
| 18 | 22.9 | 5.75 | 2.47 |
| 19 | 23.5 | 1.61 | 1.17 |
| 20 | 27.3 | 5.94 | 0.83 |
| 21 | 26.7 | 7.2 | 1.67 |
| 22 | 25.3 | 5.94 | 3.44 |
| 23 | 25.2 | 7.06 | 3.99 |
| 24 | 24.2 | 7.07 | 3.5 |
| 25 | 24.5 | 7.03 | 1.39 |
| 26 | 24.7 | 5.39 | 2.47 |
| 27 | 25.1 | 6.54 | 1.93 |
| 28 | 26.1 | 5.23 | 0.76 |
| 29 | 24.4 | 7.04 | 1.57 |
| 30 | 23.5 | 6.83 | 1.15 |
| 31 | 23.6 | 3.46 | 3.7 |

| **June** | | | |
|---|---|---|---|
| **Days** | **Ta [°C]** | **G. Rad [kWh/m²]** | **v [m/s]** |
| 1 | 22 | 5.98 | 2.09 |
| 2 | 22.1 | 3.49 | 1.78 |
| 3 | 22 | 4.74 | 2.99 |
| 4 | 20.5 | 6.4 | 3.79 |
| 5 | 21.7 | 5.79 | 2.53 |
| 6 | 21.1 | 3.15 | 1.52 |
| 7 | 21.2 | 5.66 | 1.63 |
| 8 | 20.1 | 5.82 | 0.71 |
| 9 | 21 | 4.95 | 2.4 |
| 10 | 21.4 | 6.43 | 3.48 |
| 11 | 22.2 | 6.01 | 1.66 |
| 12 | 22.6 | 5.69 | 0.6 |
| 13 | 23 | 4.89 | 1.19 |
| 14 | 22.7 | 6.51 | 2.38 |
| 15 | 21.9 | 6.49 | 4.54 |
| 16 | 22.5 | 6.24 | 1.16 |
| 17 | 20.8 | 6.39 | 1.6 |
| 18 | 22.6 | 6.25 | 3.58 |
| 19 | 25.1 | 5.66 | 2.14 |
| 20 | 24.7 | 5.45 | 1.97 |
| 21 | 24.4 | 6.43 | 1.45 |
| 22 | 23.9 | 6.3 | 1.8 |
| 23 | 23.7 | 5.53 | 0.4 |
| 24 | 23.3 | 5.22 | 1.21 |
| 25 | 24.2 | 5.53 | 1.06 |
| 26 | 22.3 | 6.03 | 1.29 |
| 27 | 21.5 | 3.61 | 1.01 |

| | | | |
|---|---|---|---|
| 28 | 22.4 | 6.54 | 4.06 |
| 29 | 21.8 | 6.7 | 2.41 |
| 30 | 21.2 | 6.74 | 7.37 |

| **July** | | | |
|---|---|---|---|
| **Days** | **Ta [°C]** | **G. Rad [kWh/m²]** | **v [m/s]** |
| 1 | 21.9 | 5.21 | 3.45 |
| 2 | 22.9 | 6.76 | 3.63 |
| 3 | 23.4 | 4.1 | 1.68 |
| 4 | 21 | 6.36 | 0.56 |
| 5 | 20.9 | 4.58 | 1.93 |
| 6 | 19.5 | 2.21 | 5.93 |
| 7 | 21.7 | 2.94 | 1.6 |
| 8 | 22.8 | 5.34 | 1.75 |
| 9 | 25.3 | 6.23 | 3.63 |
| 10 | 23.6 | 5.01 | 2.18 |
| 11 | 22.5 | 5.56 | 1.37 |
| 12 | 22.1 | 4.75 | 1.8 |
| 13 | 21.9 | 2.37 | 1.96 |
| 14 | 19.8 | 5.46 | 2.64 |
| 15 | 18.9 | 6.19 | 0.56 |
| 16 | 20 | 4.64 | 2.85 |
| 17 | 21.4 | 4.71 | 0.89 |
| 18 | 23.3 | 5.91 | 2.99 |
| 19 | 23.2 | 5.26 | 1.4 |
| 20 | 20.5 | 4.74 | 2.15 |
| 21 | 26.3 | 5.62 | 0.7 |
| 22 | 24.2 | 2.67 | 4.27 |
| 23 | 23.8 | 6.49 | 4.07 |
| 24 | 22.6 | 5.52 | 2.52 |
| 25 | 21.2 | 4.91 | 2.64 |
| 26 | 19.3 | 4.82 | 1.7 |
| 27 | 21.5 | 4.7 | 4.66 |
| 28 | 22.4 | 4.82 | 1.65 |
| 29 | 24.1 | 5.03 | 1.33 |
| 30 | 20.7 | 4.49 | 2.5 |
| 31 | 23 | 6.66 | 3.4 |

| **August** | | | |
|---|---|---|---|
| **Days** | **Ta [°C]** | **G. Rad [kWh/m²]** | **v [m/s]** |
| 1 | 21.9 | 6.08 | 2.23 |
| 2 | 21.6 | 6.94 | 5.11 |
| 3 | 20.8 | 3.66 | 2.01 |

| | | | |
|---|---|---|---|
| 4 | 19.3 | 3.51 | 0.98 |
| 5 | 21.2 | 6.28 | 0.92 |
| 6 | 21 | 6.13 | 0.4 |
| 7 | 19.2 | 2.05 | 2.11 |
| 8 | 21.7 | 3.6 | 4.37 |
| 9 | 21.4 | 3.54 | 4.03 |
| 10 | 22 | 6.16 | 2.29 |
| 11 | 22.6 | 6.03 | 4.38 |
| 12 | 23.1 | 6.14 | 3.04 |
| 13 | 22.5 | 6.61 | 0.92 |
| 14 | 22.8 | 2.21 | 3.31 |
| 15 | 22.8 | 3.92 | 2.86 |
| 16 | 22.9 | 4.06 | 1.44 |
| 17 | 23.8 | 6.3 | 1.8 |
| 18 | 25.3 | 5.34 | 1.06 |
| 19 | 25.9 | 4.91 | 2.03 |
| 20 | 24.2 | 5.65 | 2.09 |
| 21 | 23.3 | 5.59 | 1.93 |
| 22 | 22.2 | 5.21 | 2.34 |
| 23 | 22.3 | 2.51 | 1.76 |
| 24 | 23.4 | 4.14 | 1.25 |
| 25 | 24.3 | 3.81 | 0.64 |
| 26 | 23.6 | 6.54 | 1.8 |
| 27 | 24.5 | 3.12 | 4.22 |
| 28 | 24 | 6.84 | 1.89 |
| 29 | 23.7 | 4.11 | 1.43 |
| 30 | 23.9 | 4.4 | 1.08 |
| 31 | 24.7 | 6.52 | 5.46 |

| **September** | | | |
|---|---|---|---|
| **Days** | **Ta [°C]** | **G. Rad [kWh/m²]** | **v [m/s]** |
| 1 | 26.3 | 7.28 | 1.32 |
| 2 | 26.7 | 4.54 | 1.63 |
| 3 | 26.7 | 2.64 | 0.07 |
| 4 | 28 | 4.5 | 2.36 |
| 5 | 27.5 | 2.87 | 1.41 |
| 6 | 24.5 | 3.85 | 1 |
| 7 | 23.5 | 5.95 | 2.83 |
| 8 | 23.6 | 5.75 | 5.61 |
| 9 | 22.6 | 7.08 | 1.81 |
| 10 | 22.9 | 6.9 | 1.71 |
| 11 | 21.8 | 7 | 4.02 |
| 12 | 22.2 | 5.96 | 1.92 |
| 13 | 23.4 | 7.05 | 1.69 |

| | | | |
|---|---|---|---|
| 14 | 22.7 | 6.85 | 4.22 |
| 15 | 24.5 | 6.87 | 3 |
| 16 | 24.3 | 6.37 | 4.19 |
| 17 | 23.1 | 5.84 | 1.62 |
| 18 | 24 | 3.58 | 0.94 |
| 19 | 23.2 | 1.63 | 1.92 |
| 20 | 23.8 | 6.3 | 1.04 |
| 21 | 24.6 | 7.38 | 2.14 |
| 22 | 24.2 | 7.15 | 2.44 |
| 23 | 24.1 | 6.9 | 3.41 |
| 24 | 26.5 | 6.69 | 4.86 |
| 25 | 25.8 | 2.86 | 1.26 |
| 26 | 23.2 | 3.35 | 4.96 |
| 27 | 23.6 | 5.94 | 3.08 |
| 28 | 24.7 | 3.47 | 1.46 |
| 29 | 25 | 6.62 | 2.44 |
| 30 | 25.4 | 6.16 | 1.59 |

| **October** | | | |
|---|---|---|---|
| **Days** | **Ta [°C]** | **G. Rad [kWh/m²]** | **v [m/s]** |
| 1 | 25 | 7.11 | 1.2 |
| 2 | 24.3 | 6.96 | 3.76 |
| 3 | 25.5 | 6.92 | 1.99 |
| 4 | 26.1 | 6.87 | 5.13 |
| 5 | 26.8 | 6.76 | 2.1 |
| 6 | 27.2 | 6.91 | 3 |
| 7 | 27.5 | 4.75 | 3.23 |
| 8 | 26.9 | 7.25 | 3.45 |
| 9 | 27.7 | 6.94 | 2.13 |
| 10 | 29.7 | 7.09 | 4.9 |
| 11 | 30.2 | 6.17 | 2.13 |
| 12 | 29.2 | 5.55 | 1.59 |
| 13 | 28.8 | 6.68 | 0.55 |
| 14 | 28.5 | 5.78 | 1.37 |
| 15 | 28 | 7.15 | 2.56 |
| 16 | 27.1 | 5.79 | 1.92 |
| 17 | 27.4 | 5.79 | 3.08 |
| 18 | 27.3 | 6.63 | 1.8 |
| 19 | 26.5 | 5.85 | 2.63 |
| 20 | 27.8 | 3.18 | 1.44 |
| 21 | 27.8 | 4.43 | 2.94 |
| 22 | 26.7 | 5.9 | 7.15 |
| 23 | 26 | 6.46 | 1.95 |
| 24 | 26.4 | 6.47 | 4.2 |

| | | | |
|---|---|---|---|
| 25 | 25.6 | 5.08 | 1.9 |
| 26 | 24.7 | 5.73 | 1.6 |
| 27 | 25.2 | 5.63 | 0.87 |
| 28 | 23.9 | 6.02 | 1 |
| 29 | 25.8 | 6.56 | 0.88 |
| 30 | 26.2 | 6.16 | 2.74 |
| 31 | 25.7 | 6.68 | 2.14 |

| **November** | | | |
|---|---|---|---|
| **Days** | **Ta [°C]** | **G. Rad [kWh/m²]** | **v [m/s]** |
| 1 | 24.6 | 6.46 | 3 |
| 2 | 25 | 5.92 | 2.21 |
| 3 | 25.4 | 6.7 | 3.85 |
| 4 | 25.6 | 6.58 | 3.11 |
| 5 | 26.3 | 6.24 | 3.1 |
| 6 | 26.5 | 6.44 | 2.07 |
| 7 | 26.6 | 6.12 | 0.8 |
| 8 | 27.1 | 6.23 | 1.33 |
| 9 | 27.4 | 5.97 | 2.7 |
| 10 | 29.2 | 6.52 | 1.07 |
| 11 | 30 | 6.08 | 4.4 |
| 12 | 26 | 6.03 | 3.32 |
| 13 | 27.2 | 6.68 | 2.57 |
| 14 | 25.1 | 6.14 | 1.09 |
| 15 | 26.7 | 6.31 | 1.9 |
| 16 | 27.4 | 5.51 | 1.69 |
| 17 | 26.5 | 6.24 | 3.47 |
| 18 | 27 | 6.43 | 3.53 |
| 19 | 30.6 | 6.23 | 4.26 |
| 20 | 29.5 | 6.1 | 2.35 |
| 21 | 27.8 | 4.98 | 1.35 |
| 22 | 28.7 | 5.1 | 1.97 |
| 23 | 28.9 | 5.87 | 3.18 |
| 24 | 26.9 | 6.55 | 2.35 |
| 25 | 28.2 | 6.46 | 2.67 |
| 26 | 26.9 | 6.63 | 0.36 |
| 27 | 25.6 | 6.39 | 0.99 |
| 28 | 26.1 | 6.41 | 4.21 |
| 29 | 25.8 | 6.25 | 1.95 |
| 30 | 26.2 | 5.92 | 1.28 |

| Decembers | | | |
|---|---|---|---|
| Days | Ta [°C] | G. Rad [kWh/m²] | v [m/s] |
| 1 | 27.1 | 5.97 | 1.21 |
| 2 | 25.8 | 6.36 | 2.34 |
| 3 | 28.6 | 6.18 | 0.81 |
| 4 | 28.3 | 6.04 | 0.72 |
| 5 | 26.9 | 6.26 | 1.95 |
| 6 | 26.1 | 6.02 | 2.33 |
| 7 | 26.2 | 6.01 | 2.11 |
| 8 | 26.7 | 6.04 | 0.67 |
| 9 | 25.6 | 6.03 | 0.88 |
| 10 | 25.9 | 5.04 | 1.07 |
| 11 | 24.8 | 5.67 | 1.85 |
| 12 | 26.6 | 5.54 | 3 |
| 13 | 25.3 | 6.19 | 2.52 |
| 14 | 27.4 | 4.62 | 4.12 |
| 15 | 27.6 | 5.71 | 0.76 |
| 16 | 29.3 | 6.01 | 2.39 |
| 17 | 27.3 | 6.19 | 2.4 |
| 18 | 28.9 | 5.91 | 2.14 |
| 19 | 28 | 6.26 | 3.37 |
| 20 | 27.8 | 6.27 | 1.15 |
| 21 | 24.5 | 5.87 | 0.91 |
| 22 | 26.4 | 5.67 | 1.47 |
| 23 | 25 | 5.82 | 1.83 |
| 24 | 23.7 | 6.13 | 0.87 |
| 25 | 22.6 | 5.98 | 1.86 |
| 26 | 23.1 | 5.58 | 1.37 |
| 27 | 23.9 | 5.31 | 1.93 |
| 28 | 24.2 | 5.85 | 1.55 |
| 29 | 25.1 | 4.88 | 3.27 |
| 30 | 25.4 | 6.1 | 1.6 |
| 31 | 24.6 | 5.76 | 1.43 |

Table 11. Hourly climate data collected for a typical day of each month

| January | | | |
|---|---|---|---|
| Hours | Ta [°C] | G. Rad [kW/m²] | v [m/s] |
| 1 | 20.9 | 0 | 1 |
| 2 | 20.1 | 0 | 1 |
| 3 | 19.3 | 0 | 2 |
| 4 | 18.9 | 0 | 1.3 |
| 5 | 18.5 | 0 | 0.3 |
| 6 | 18.2 | 0 | 0.2 |

| | | | |
|---|---|---|---|
| 7 | 18.2 | 0 | 0.1 |
| 8 | 19.6 | 0.103 | 0.7 |
| 9 | 21.8 | 0.298 | 1.6 |
| 10 | 24.2 | 0.483 | 2.8 |
| 11 | 26.5 | 0.632 | 0.9 |
| 12 | 28.4 | 0.729 | 2.5 |
| 13 | 30 | 0.769 | 2 |
| 14 | 31 | 0.734 | 3.3 |
| 15 | 31.5 | 0.639 | 6.4 |
| 16 | 31.5 | 0.491 | 4.9 |
| 17 | 30.7 | 0.31 | 3.8 |
| 18 | 29.2 | 0.112 | 1.5 |
| 19 | 27.6 | 0.001 | 1 |
| 20 | 26.5 | 0 | 0.3 |
| 21 | 25.5 | 0 | 0.5 |
| 22 | 24.4 | 0 | 1.3 |
| 23 | 23.4 | 0 | 1.8 |
| 24 | 22.3 | 0 | 1.5 |

| **February** | | | |
|---|---|---|---|
| **Hours** | **Ta [°C]** | **G. Rad [kW/m²]** | **v [m/s]** |
| 1 | 19.4 | 0 | 0.5 |
| 2 | 18.4 | 0 | 0.6 |
| 3 | 17.4 | 0 | 1.1 |
| 4 | 16.9 | 0 | 0.7 |
| 5 | 16.4 | 0 | 0.1 |
| 6 | 16.1 | 0 | 0.1 |
| 7 | 16 | 0.001 | 0.3 |
| 8 | 17.9 | 0.136 | 0.5 |
| 9 | 20.9 | 0.39 | 0.6 |
| 10 | 24 | 0.636 | 0.7 |
| 11 | 27.1 | 0.842 | 0.7 |
| 12 | 29.7 | 0.965 | 0.6 |
| 13 | 31.7 | 1.011 | 0.2 |
| 14 | 33.1 | 0.978 | 2 |
| 15 | 33.8 | 0.866 | 2.3 |
| 16 | 33.9 | 0.68 | 3 |
| 17 | 32.9 | 0.443 | 4.5 |
| 18 | 31.1 | 0.186 | 5.4 |
| 19 | 28.9 | 0.003 | 4 |
| 20 | 27.8 | 0 | 2 |
| 21 | 26.6 | 0 | 1.3 |
| 22 | 25.5 | 0 | 1.5 |
| 23 | 24.4 | 0 | 2.6 |

| | | | |
|---|---|---|---|
| 24 | 23.3 | 0 | 1.7 |

| March | | | |
|---|---|---|---|
| **Hours** | **Ta [°C]** | **G. Rad [kW/m²]** | **v [m/s]** |
| 1 | 22.3 | 0 | 1.6 |
| 2 | 21.3 | 0 | 1.2 |
| 3 | 20.2 | 0 | 2.9 |
| 4 | 19.7 | 0 | 1.4 |
| 5 | 19.2 | 0 | 0.4 |
| 6 | 18.8 | 0 | 0.6 |
| 7 | 18.8 | 0.003 | 0.2 |
| 8 | 20.8 | 0.17 | 0.7 |
| 9 | 23.5 | 0.425 | 2.2 |
| 10 | 26.2 | 0.657 | 1.9 |
| 11 | 28.7 | 0.847 | 4.8 |
| 12 | 30.9 | 0.974 | 3.2 |
| 13 | 32.6 | 1.015 | 3.2 |
| 14 | 33.8 | 0.983 | 2.9 |
| 15 | 34.3 | 0.859 | 1.6 |
| 16 | 34.3 | 0.672 | 1.6 |
| 17 | 33.4 | 0.44 | 1.6 |
| 18 | 31.7 | 0.186 | 1.1 |
| 19 | 29.8 | 0.005 | 1.4 |
| 20 | 28.8 | 0 | 2.2 |
| 21 | 27.8 | 0 | 0.6 |
| 22 | 26.8 | 0 | 0.2 |
| 23 | 25.9 | 0 | 0.7 |
| 24 | 24.9 | 0 | 1.1 |

| April | | | |
|---|---|---|---|
| **Hours** | **Ta [°C]** | **G. Rad [kW/m²]** | **v [m/s]** |
| 1 | 21.8 | 0 | 1.6 |
| 2 | 21.2 | 0 | 1.9 |
| 3 | 20.5 | 0 | 5.3 |
| 4 | 20.1 | 0 | 3 |
| 5 | 19.8 | 0 | 6.7 |
| 6 | 19.6 | 0 | 4.1 |
| 7 | 19.8 | 0.012 | 1.8 |
| 8 | 21.6 | 0.179 | 2.1 |
| 9 | 23.6 | 0.37 | 2.6 |
| 10 | 25.6 | 0.557 | 3.8 |

| | | | |
|---|---|---|---|
| 11 | 27.4 | 0.703 | 7.5 |
| 12 | 29 | 0.802 | 7 |
| 13 | 30.2 | 0.832 | 4.8 |
| 14 | 30.9 | 0.765 | 2.4 |
| 15 | 31.2 | 0.659 | 3.4 |
| 16 | 31 | 0.51 | 9.1 |
| 17 | 30.3 | 0.338 | 9.1 |
| 18 | 29.1 | 0.138 | 4.8 |
| 19 | 27.7 | 0.002 | 1.8 |
| 20 | 26.7 | 0 | 1.8 |
| 21 | 25.7 | 0 | 0.9 |
| 22 | 24.7 | 0 | 0.4 |
| 23 | 23.8 | 0 | 0.9 |
| 24 | 22.8 | 0 | 0.5 |

| **May** | | | |
|---|---|---|---|
| **Hours** | **Ta [°C]** | **G. Rad [kW/m²]** | **v [m/s]** |
| 1 | 19.6 | 0 | 6.7 |
| 2 | 19.4 | 0 | 4.7 |
| 3 | 19.2 | 0 | 6.7 |
| 4 | 19.1 | 0 | 3.7 |
| 5 | 19 | 0 | 3.2 |
| 6 | 19 | 0 | 2.8 |
| 7 | 19.3 | 0.014 | 3.7 |
| 8 | 21 | 0.159 | 7.7 |
| 9 | 22.7 | 0.311 | 6.7 |
| 10 | 24.3 | 0.436 | 7.7 |
| 11 | 26 | 0.592 | 6.2 |
| 12 | 27.4 | 0.653 | 4.7 |
| 13 | 28.5 | 0.69 | 3.7 |
| 14 | 29.1 | 0.624 | 2.3 |
| 15 | 29.5 | 0.552 | 3.4 |
| 16 | 29.3 | 0.396 | 3.7 |
| 17 | 28.6 | 0.246 | 3.2 |
| 18 | 27.5 | 0.095 | 2.8 |
| 19 | 26.3 | 0.002 | 4.3 |
| 20 | 25.4 | 0 | 2.5 |
| 21 | 24.5 | 0 | 1.9 |
| 22 | 23.5 | 0 | 1 |
| 23 | 22.6 | 0 | 1.8 |
| 24 | 21.7 | 0 | 1.3 |

| June | | | |
|---|---|---|---|
| **Hours** | **Ta [°C]** | **G. Rad [kW/m²]** | **v [m/s]** |
| 1 | 18.6 | 0 | 1 |
| 2 | 17.9 | 0 | 0.4 |
| 3 | 17.2 | 0 | 0.6 |
| 4 | 16.8 | 0 | 0.4 |
| 5 | 16.5 | 0 | 0.2 |
| 6 | 16.2 | 0 | 0.2 |
| 7 | 16.5 | 0.017 | 0.1 |
| 8 | 18.8 | 0.223 | 0.2 |
| 9 | 21 | 0.415 | 1.2 |
| 10 | 23.1 | 0.6 | 1.4 |
| 11 | 24.7 | 0.686 | 0.6 |
| 12 | 26.1 | 0.758 | 0.9 |
| 13 | 26.9 | 0.719 | 3.4 |
| 14 | 27.6 | 0.755 | 3.4 |
| 15 | 28.1 | 0.729 | 3.1 |
| 16 | 28.1 | 0.56 | 1.4 |
| 17 | 27.4 | 0.375 | 0.6 |
| 18 | 26.2 | 0.165 | 1.2 |
| 19 | 24.7 | 0.009 | 2.8 |
| 20 | 23.7 | 0 | 4.2 |
| 21 | 22.8 | 0 | 2 |
| 22 | 21.9 | 0 | 3.7 |
| 23 | 21 | 0 | 3.4 |
| 24 | 20.1 | 0 | 3.4 |

| July | | | |
|---|---|---|---|
| **Hours** | **Ta [°C]** | **G. Rad [kW/m²]** | **v [m/s]** |
| 1 | 18.3 | 0 | 0.8 |
| 2 | 17.8 | 0 | 0.5 |
| 3 | 17.2 | 0 | 0.4 |
| 4 | 16.9 | 0 | 0.3 |
| 5 | 16.7 | 0 | 0.1 |
| 6 | 16.5 | 0 | 0 |
| 7 | 16.7 | 0.011 | 0 |
| 8 | 18.2 | 0.142 | 0 |
| 9 | 19.9 | 0.302 | 0.5 |
| 10 | 21.8 | 0.474 | 0.6 |
| 11 | 23.4 | 0.581 | 1 |
| 12 | 24.7 | 0.631 | 1 |
| 13 | 25.7 | 0.681 | 2 |
| 14 | 26.3 | 0.614 | 2.2 |
| 15 | 26.6 | 0.525 | 3.8 |

| | | | |
|---|---|---|---|
| 16 | 26.4 | 0.405 | 2.9 |
| 17 | 25.7 | 0.245 | 2.2 |
| 18 | 24.6 | 0.097 | 2.2 |
| 19 | 23.3 | 0.003 | 0.1 |
| 20 | 22.6 | 0 | 0.1 |
| 21 | 21.9 | 0 | 0.3 |
| 22 | 21.2 | 0 | 0.1 |
| 23 | 20.5 | 0 | 0.1 |
| 24 | 19.7 | 0 | 0.2 |

| **August** | | | |
|---|---|---|---|
| **Hours** | **Ta [°C]** | **G. Rad [kW/m²]** | **v [m/s]** |
| 1 | 20.7 | 0 | 1 |
| 2 | 20.1 | 0 | 1.9 |
| 3 | 19.6 | 0 | 3.1 |
| 4 | 19.3 | 0 | 2.2 |
| 5 | 19 | 0 | 2.4 |
| 6 | 18.8 | 0 | 2.4 |
| 7 | 19.3 | 0.022 | 2.2 |
| 8 | 21.4 | 0.223 | 1.7 |
| 9 | 23.5 | 0.422 | 1.1 |
| 10 | 24.6 | 0.43 | 1.1 |
| 11 | 26 | 0.607 | 0.5 |
| 12 | 27.2 | 0.697 | 0.4 |
| 13 | 28 | 0.664 | 0.9 |
| 14 | 27.6 | 0.34 | 1.1 |
| 15 | 27.3 | 0.35 | 1.7 |
| 16 | 26.5 | 0.184 | 1.2 |
| 17 | 25.5 | 0.088 | 0.5 |
| 18 | 24.5 | 0.03 | 0.9 |
| 19 | 23.6 | 0.004 | 0.8 |
| 20 | 22.9 | 0 | 1.1 |
| 21 | 22.2 | 0 | 1 |
| 22 | 21.5 | 0 | 2 |
| 23 | 20.9 | 0 | 1.7 |
| 24 | 20.2 | 0 | 1.7 |

| **September** | | | |
|---|---|---|---|
| **Hours** | **Ta [°C]** | **G. Rad [kW/m²]** | **v [m/s]** |
| 1 | 19.6 | 0 | 6.5 |
| 2 | 18.9 | 0 | 2.8 |
| 3 | 18.3 | 0 | 3.9 |
| 4 | 17.9 | 0 | 3.9 |

| | | | |
|---|---|---|---|
| 5 | 17.5 | 0 | 3.5 |
| 6 | 17.3 | 0 | 2.3 |
| 7 | 17.6 | 0.015 | 3.2 |
| 8 | 20 | 0.217 | 2.3 |
| 9 | 22.6 | 0.459 | 4.5 |
| 10 | 25.2 | 0.671 | 5.1 |
| 11 | 27.5 | 0.839 | 5.5 |
| 12 | 29.4 | 0.932 | 4.8 |
| 13 | 30.8 | 0.967 | 3.7 |
| 14 | 31.7 | 0.903 | 4.2 |
| 15 | 32.1 | 0.786 | 2.1 |
| 16 | 31.9 | 0.593 | 1.2 |
| 17 | 30.8 | 0.361 | 3 |
| 18 | 29.2 | 0.127 | 2.3 |
| 19 | 27.4 | 0.001 | 1.6 |
| 20 | 26.4 | 0 | 1.2 |
| 21 | 25.3 | 0 | 1.3 |
| 22 | 24.3 | 0 | 1.3 |
| 23 | 23.2 | 0 | 0.5 |
| 24 | 22.2 | 0 | 1.3 |

| **October** | | | |
|---|---|---|---|
| **Hours** | **Ta [°C]** | **G. Rad [kW/m²]** | **v [m/s]** |
| 1 | 24.3 | 0 | 1.1 |
| 2 | 23.4 | 0 | 1.5 |
| 3 | 22.5 | 0 | 2.2 |
| 4 | 22.1 | 0 | 1.8 |
| 5 | 21.6 | 0 | 1.8 |
| 6 | 21.3 | 0 | 1.8 |
| 7 | 21.7 | 0.02 | 1.5 |
| 8 | 24.1 | 0.255 | 2.4 |
| 9 | 26.6 | 0.51 | 2 |
| 10 | 29 | 0.732 | 2.7 |
| 11 | 31 | 0.893 | 4.3 |
| 12 | 32.7 | 0.987 | 4.6 |
| 13 | 34 | 1.004 | 3 |
| 14 | 34.7 | 0.937 | 2.6 |
| 15 | 35 | 0.794 | 3.9 |
| 16 | 34.6 | 0.588 | 3.4 |
| 17 | 33.5 | 0.335 | 3.9 |
| 18 | 31.9 | 0.093 | 5.2 |
| 19 | 30.2 | 0 | 4.6 |
| 20 | 29.3 | 0 | 2.4 |
| 21 | 28.3 | 0 | 2 |

| | | | |
|---|---|---|---|
| 22 | 27.3 | 0 | 1.1 |
| 23 | 26.3 | 0 | 0.5 |
| 24 | 25.4 | 0 | 1.1 |

| November | | | |
|---|---|---|---|
| **Hours** | **Ta [°C]** | **G. Rad [kW/m²]** | **v [m/s]** |
| 1 | 23.4 | 0 | 1.5 |
| 2 | 22.3 | 0 | 4.7 |
| 3 | 21.1 | 0 | 4.1 |
| 4 | 20.5 | 0 | 3.5 |
| 5 | 19.9 | 0 | 1.8 |
| 6 | 19.5 | 0 | 0.7 |
| 7 | 19.6 | 0.012 | 0.9 |
| 8 | 21.6 | 0.211 | 0.5 |
| 9 | 23.8 | 0.44 | 0.1 |
| 10 | 25.9 | 0.643 | 0.2 |
| 11 | 27.7 | 0.796 | 1 |
| 12 | 29.2 | 0.879 | 0.5 |
| 13 | 30.3 | 0.88 | 0.5 |
| 14 | 30.8 | 0.805 | 0.4 |
| 15 | 31 | 0.683 | 0.4 |
| 16 | 30.5 | 0.496 | 1.4 |
| 17 | 29.5 | 0.266 | 1.6 |
| 18 | 27.9 | 0.032 | 0.9 |
| 19 | 27 | 0 | 0.9 |
| 20 | 26.1 | 0 | 0.1 |
| 21 | 25.2 | 0 | 0.1 |
| 22 | 24.3 | 0 | 0.2 |
| 23 | 23.4 | 0 | 0.2 |
| 24 | 22.5 | 0 | 0 |

| December | | | |
|---|---|---|---|
| **Hours** | **Ta [°C]** | **G. Rad [kW/m²]** | **v [m/s]** |
| 1 | 22.5 | 0 | 0.3 |
| 2 | 21.9 | 0 | 0.6 |
| 3 | 21.2 | 0 | 0.6 |
| 4 | 20.9 | 0 | 1 |
| 5 | 20.6 | 0 | 0.5 |
| 6 | 20.3 | 0 | 0.8 |
| 7 | 20.5 | 0.006 | 0.3 |
| 8 | 22.6 | 0.189 | 0.2 |
| 9 | 25 | 0.398 | 1.3 |
| 10 | 27.2 | 0.57 | 2.4 |

| | | | |
|---|---|---|---|
| 11 | 29.7 | 0.809 | 1 |
| 12 | 31.3 | 0.803 | 0.7 |
| 13 | 32 | 0.667 | 1.6 |
| 14 | 32.4 | 0.628 | 1.3 |
| 15 | 32.2 | 0.461 | 0.8 |
| 16 | 31.2 | 0.292 | 0.7 |
| 17 | 30.1 | 0.172 | 1.7 |
| 18 | 28.7 | 0.049 | 2.6 |
| 19 | 27.5 | 0 | 3.2 |
| 20 | 26.5 | 0 | 1.4 |
| 21 | 25.6 | 0 | 0.6 |
| 22 | 24.7 | 0 | 1 |
| 23 | 23.7 | 0 | 0.3 |
| 24 | 22.8 | 0 | 0.7 |

# Appendix B

## T*SOL Pro 5.5 Solar Thermal System Software Programme

*Evacuated tube collector specifications*

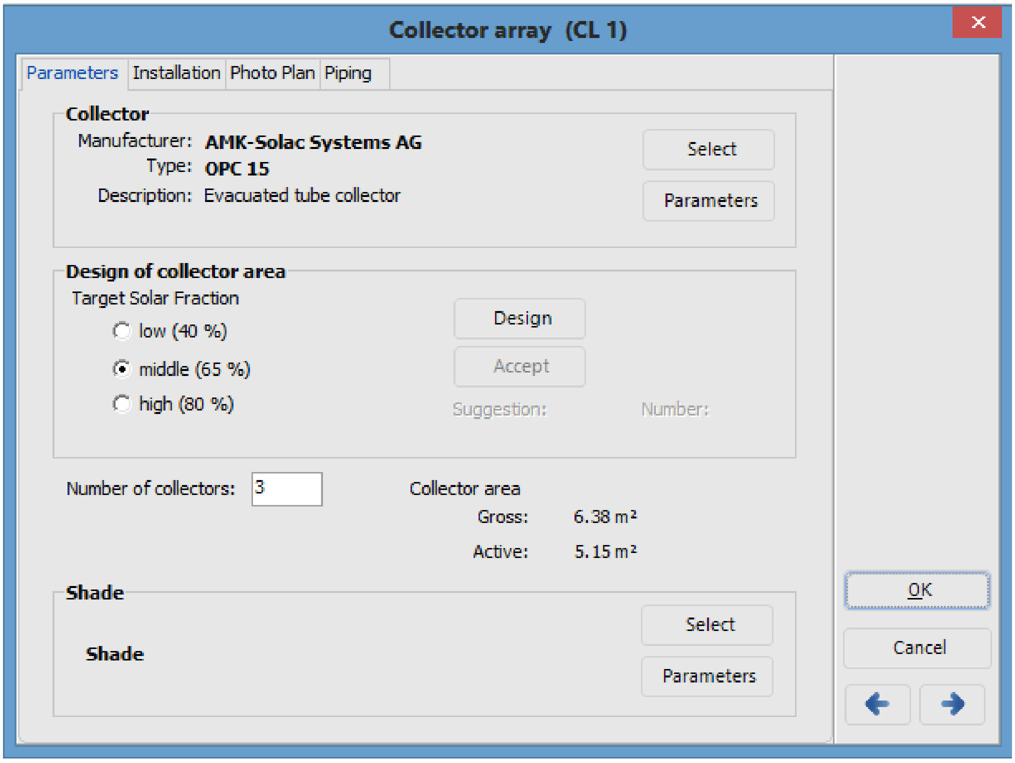


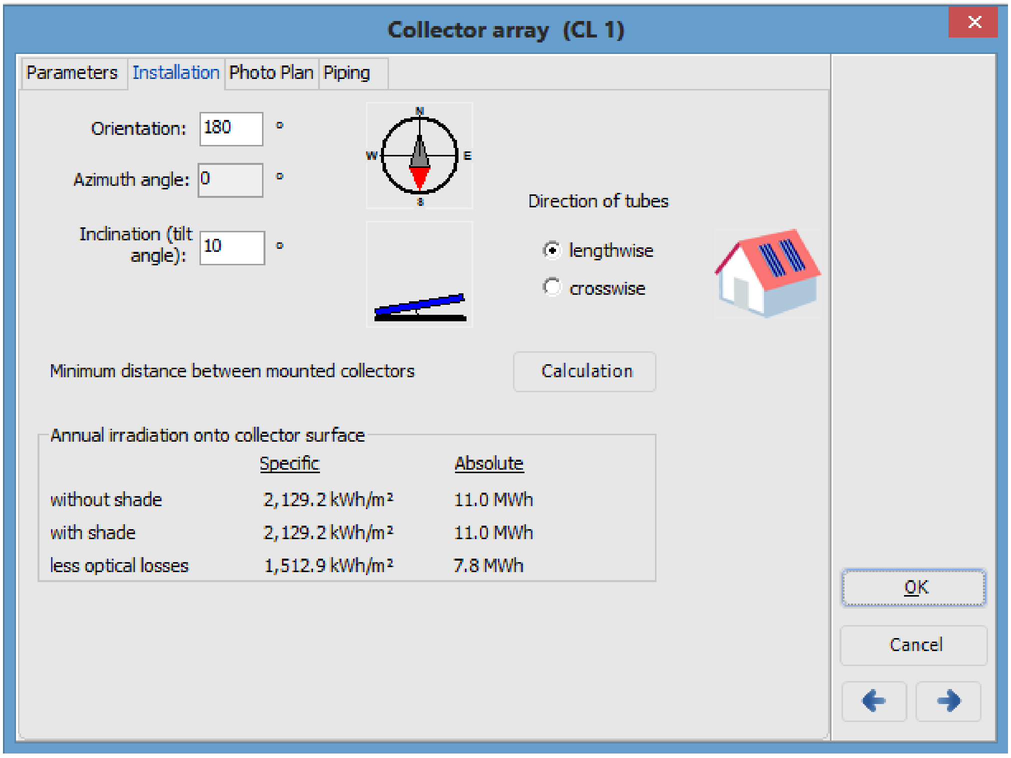

*Flat plate collector specifications*

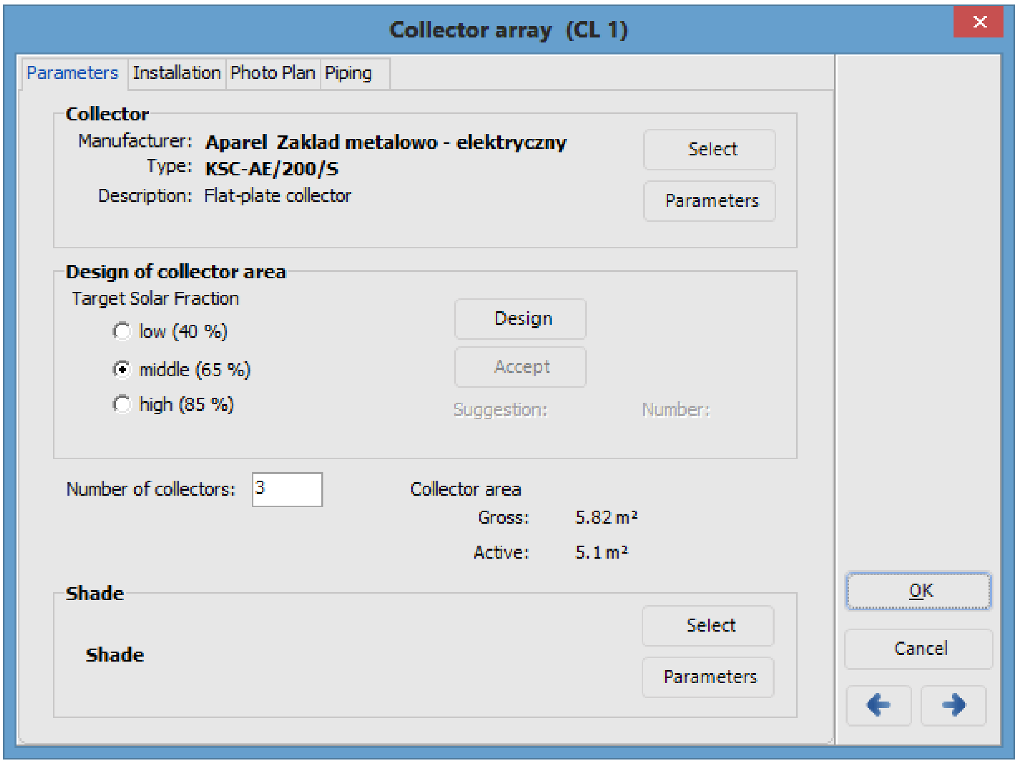


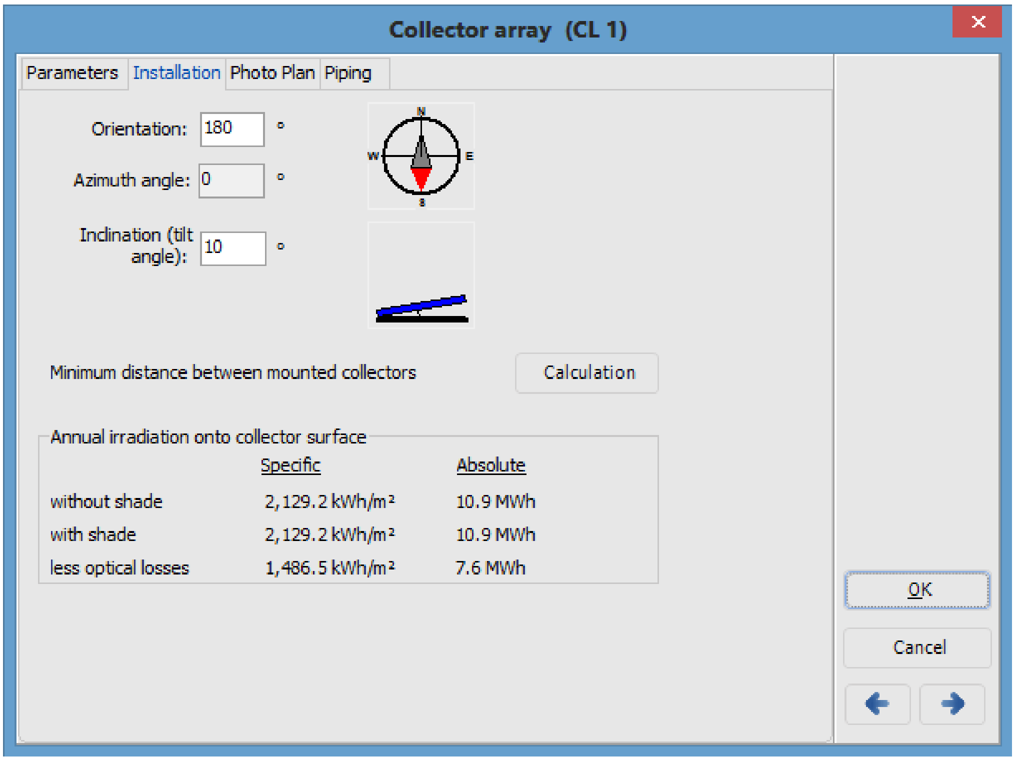

*Heat transfer fluid characteristics*

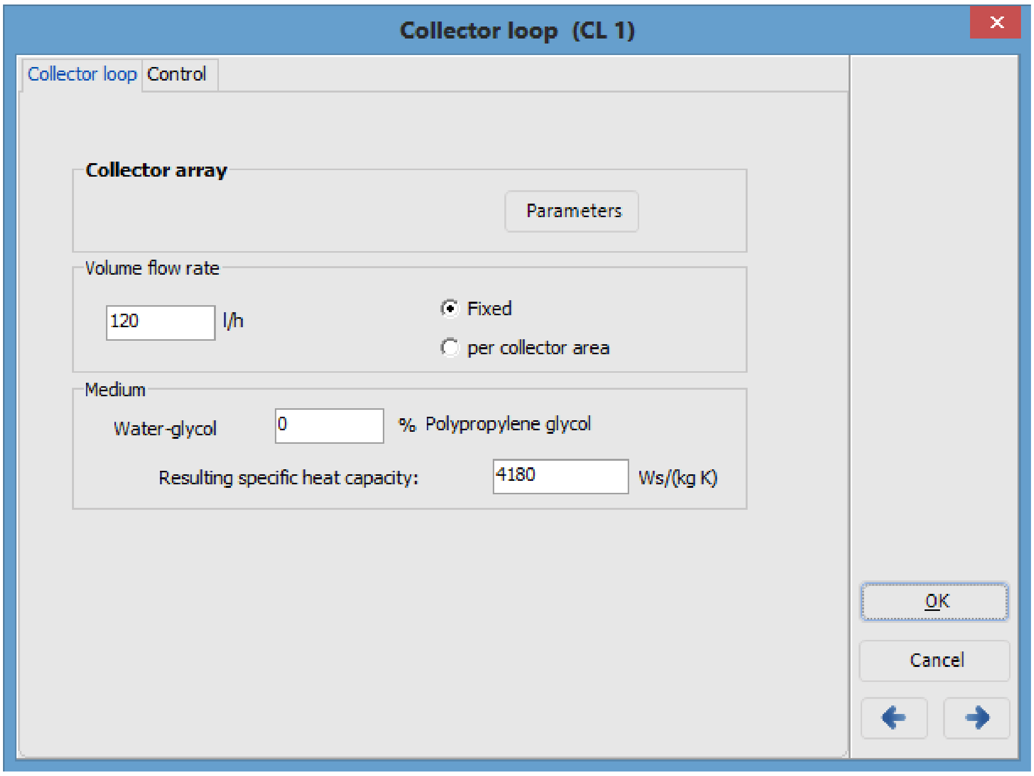


*Collector array piping and installation specification*

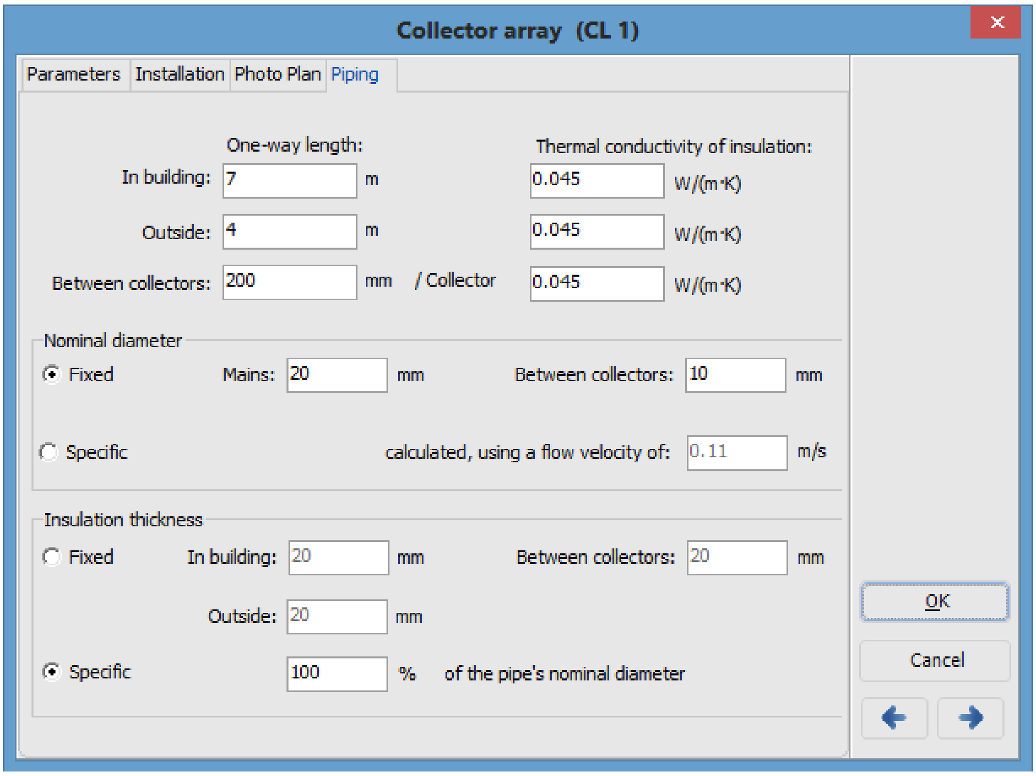

*DHW consumption profile*

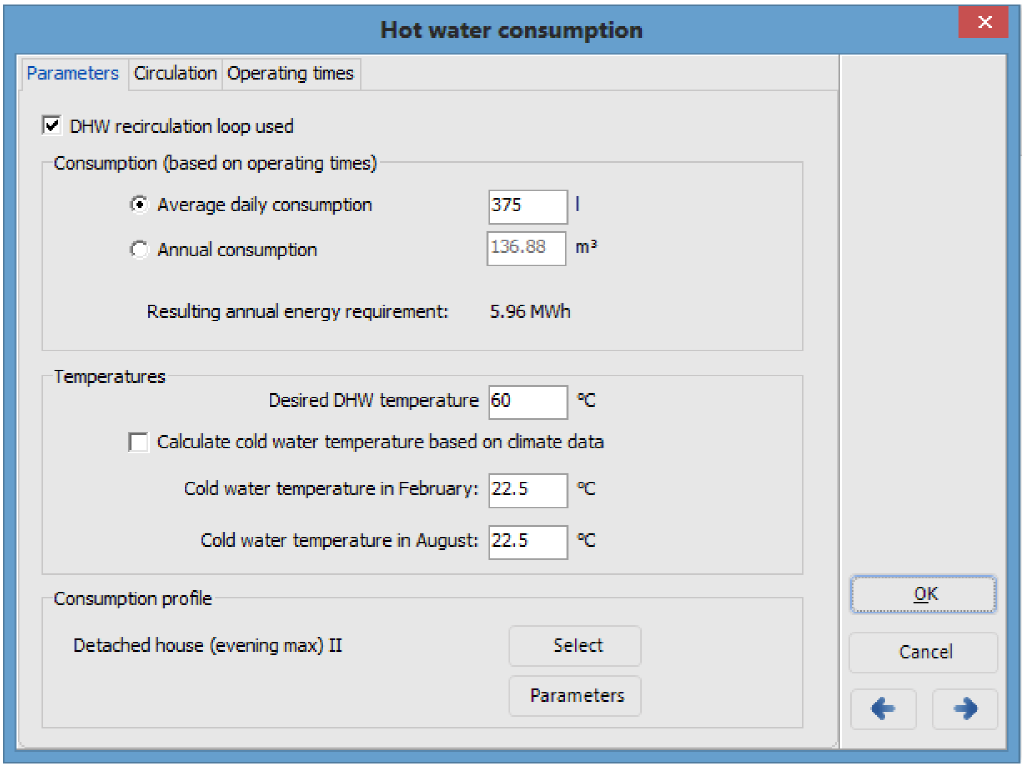


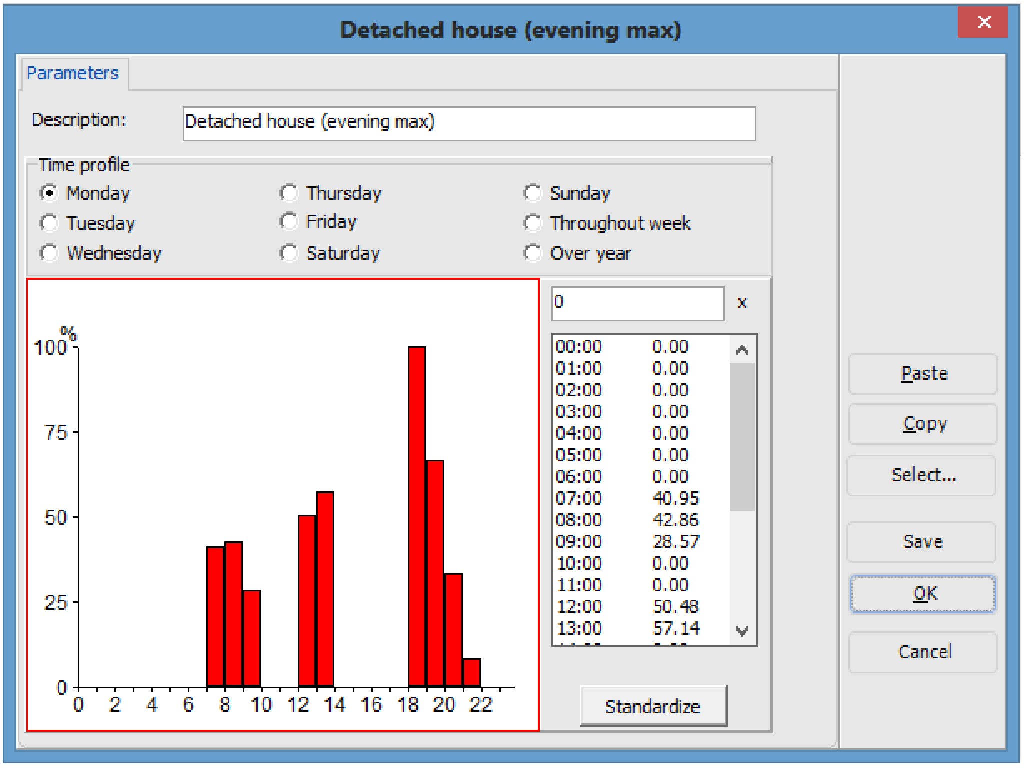

*Storage tank specifications*

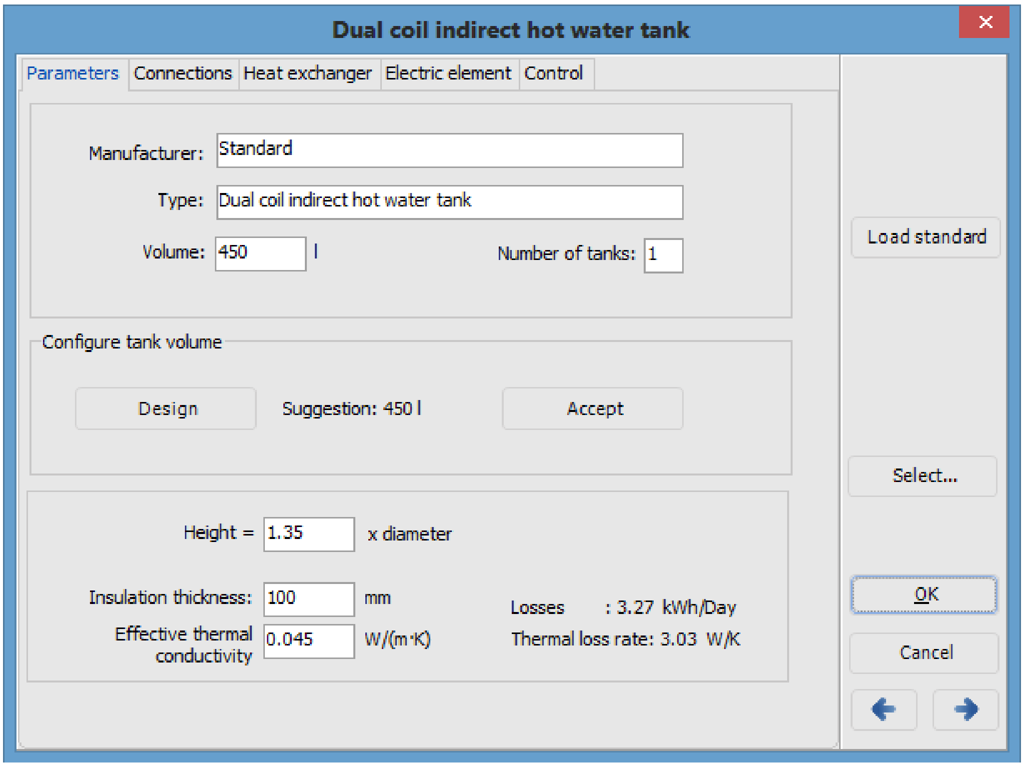


The results tool bar gives the summary of the SWH system (project report)